Journal of Medicinal Chemistry

Article

Discovery of a Furanopyrimidine-Based Epidermal Growth Factor Receptor Inhibitor (DBPR112) as a Clinical Candidate for the Treatment of Non-Small Cell Lung Cancer

Shu-Yu Lin, Yung Chang Hsu, Yi-Hui Peng, Yi-Yu Ke, Wen-Hsing Lin, Hsu-Yi Sun, Fu-Ming Kuo, Pei-Yi Chen, Tzu-Wen Lien, Chun-Hwa Chen, Chang-Ying Chu, Sing-Yi Wang, Kai-Chia Yeh, Ching-Ping Chen, Tsu-An Hsu, Suying Wu, Teng-Kuang Yeh, Chiung-Tong Chen, and Hsing-Pang Hsieh

J. Med. Chem., **Just Accepted Manuscript** • DOI: 10.1021/acs.jmedchem.9b00722 • Publication Date (Web): 27 Sep 2019

is published by the American Chemical Society. 1155 Sixteenth Street N.W., Washington, DC 20036

Discovery of a Furanopyrimidine-Based Epidermal Growth Factor Receptor Inhibitor (DBPR112) as a Clinical Candidate for the Treatment of Non-Small Cell Lung Cancer

Shu-Yu Lin,[†] Yung Chang Hsu,[†] Yi-Hui Peng,[†] Yi-Yu Ke,[†] Wen-Hsing Lin,[†] Hsu-Yi Sun,[†] Fu-Ming Kuo,[†] Pei-Yi Chen,[†] Tzu-Wen Lien,[†] Chun-Hwa Chen,[†] Chang-Ying Chu,[†] Sing-Yi Wang,[†] Kai-Chia Yeh,[†] Ching-Ping Chen,[†] Tsu-An Hsu,[†] Su-Ying Wu,[†] Teng-Kuang Yeh,[†] Chiung-Tong Chen,[†] and Hsing-Pang Hsieh*[,†,‡]

[†] *Institute of Biotechnology and Pharmaceutical Research, National Health Research Institutes, 35 Keyan Road, Zhunan, Miaoli County 35053, Taiwan, R.O.C.*
[‡]*Department of Chemistry, National Tsing Hua University, Hsinchu 30013, Taiwan, R.O.C.*

Abstract

EGFR-targeted therapy in NSCLC represents a breakthrough in the field of precision medicine. Previously, we have identified a lead compound, furanopyrimidine **2**, which contains a (*S*)-2-phenylglycinol structure as a key fragment to inhibit EGFR. However, compound **2** showed high clearance and poor oral bioavailability in its pharmacokinetics studies. In this work, we optimized compound **2** by scaffold hopping and exploiting the potent inhibitory activity of various warhead groups to obtain a clinical candidate, **78** (DBPR112), which not only displayed a potent inhibitory activity against $EGFR^{L858R/T790M}$ double mutations, but also exhibited 10-fold potency better than 3rd generation inhibitor, osimertinib, against EGFR and HER2 exon 20 insertion mutations. Overall, pharmacokinetic improvement through lead-to-candidate optimization yielded 4-fold oral AUC better that afatinib along with F = 41.5%, an encouraging safety profile, and significant antitumor efficacy in *in vivo* xenograft models. DBPR112 is currently undergoing phase 1 clinical trial in Taiwan.

INTRODUCTION

Lung cancer has the highest rate of morbidity and mortality among various cancer types, being responsible for over 1.69 million deaths per year.[1,2] Approximately 80–85% of the lung cancer patients diagnosed present non-small cell lung cancer (NSCLC).[3,4] Mutations in the epidermal growth factor receptor (EGFR) have been observed in ~50% of NSCLC patients, in particular, in East Asian patients.[4–6] The EGFR exon 19 deletions or exon 21 (L858R) substitution mutations constitute 90% of all EGFR-activating mutations.[3,7]

The first generation EGFR-targeted inhibitors, gefitinib and erlotinib, were approved by US FDA in 2003[8] and 2004 to treat mutation-positive patients.[9] Even though the two drugs showed remarkable objective response rates in EGFR-mutant NSCLC patients,[10.11] resistance can be acquired due to a secondary T790M mutation after treatment.[12,13] More recently, the irreversible second-generation EGFR tyrosine kinase inhibitor (TKI) afatinib was developed. It contains an acrylamide moiety that can undergo covalent interaction with Cys797 at the active site to enhance the binding affinity and prolong progression-free survival.[14] FDA initially approved afatinib in 2013[15] and broadened its indication in 2018 for patients with NSCLC.[16] However, afatinib showed potent activity against the wild-type (WT) EGFR, resulting in toxicity and serious adverse effects.[17,18] Very recently, AstraZeneca developed the selective covalent EGFR inhibitor AZD9291 (osimertinib), which received regular approval in 2017 for EGFR-T790M-mutation-positive NSCLC patients that showed cancer progression on EGFR TKI therapy.[19,20]

Osimertinib also has been approved by FDA as a frontline treatment in 2018. [21] However, the cost for a one-month treatment of osimertinib is $12,750 USD,[22] and several studies have revealed that patients acquire resistance after clinical use.[23–25] On September 27, 2018, FDA approved dacomitinib for the first-line treatment of metastatic NSCLC patients.[26,27] Dacomitinib is orally irreversible second-generation EGFR-TKI same as afatinib.[26]

In a previous effort to develop EGFR inhibitors, we rapidly constructed a furanopyrimidine kinase-targeted library and screened it for Aurora and EGFR kinase activities. And we identified compound **1** with (*S*)-2-phenylglycinol moiety as a potent WT EGFR inhibitor, with an IC_{50} value of 223 nM and no Aurora kinase inhibition. The docking of **1** into EGFR revealed a possible enhancement of the EGFR kinase activity through the introduction of a Michael acceptor group on the 3-position of the furan ring.[28] Based on this, we introduced an acrylamide group as a Michael acceptor, resulting in compound **2**,[28] which showed potent *in vitro* activity in both wild and mutant EGFR kinases and potent anti-proliferative activity against HCC827 lung cancer cells. In addition, since the DFG (Asp-Phe-Gly) motif plays an important role in regulating the kinase activity of EPGR,[29–31] we prepared compound **3** by structure-based drug design (SBDD), which is able to interact with the DFG motif by H-bonding and salt bridge formation.[32] The *N*,*N*-dimethylamino tail of **3** moves toward the DFG motif and forms a salt bridge with the side chain of Asp855, which greatly contributes to its potency against EGFR.[32]

In this work, we apply SBDD to guide the optimization of lead compound **2** and perform intensive lead-to-candidate optimization to identify promising candidate into the next development stage. As a result of this study, we hybridized the characteristic moieties of **2** and **3** to identify the EGFR-targeted drug candidate DBPR112 (Figure 1). DBPR112 has received investigational new drug (IND) application approval from US FDA (NCT03246854) in 2016 and Taiwan FDA in 2017 and is currently ongoing phase I clinical trials in Taiwan.[33]

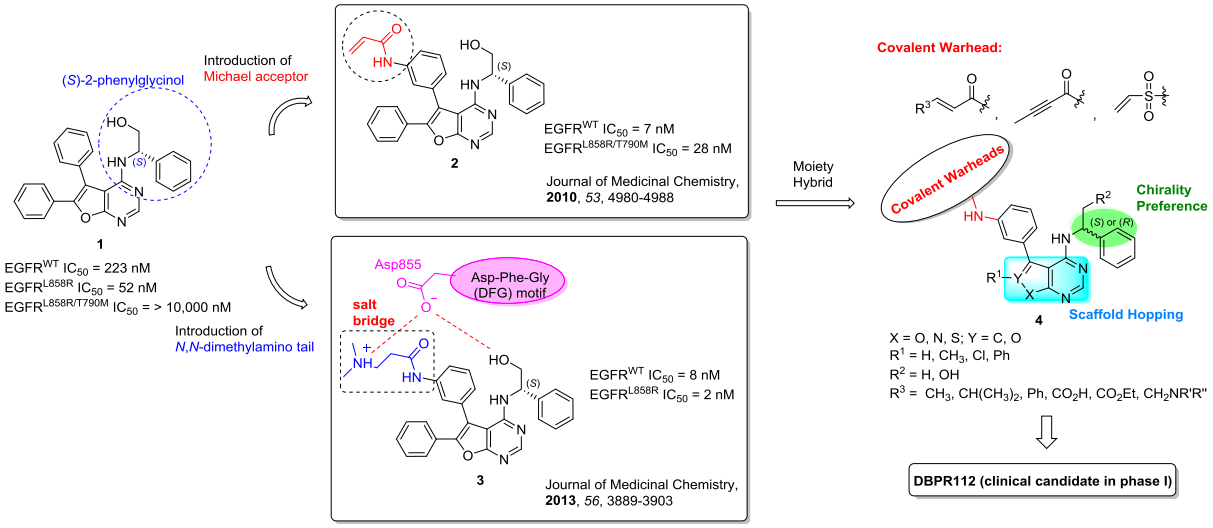

Figure 1. EGFR inhibitors design strategy from initial hit compound **1**.

RESULTS AND DISCUSSION

Binding Mode Analysis of Compound 2

The crystalline structure of EGFR kinase complex with **1** (PDB ID 4JQ7) was used to initiate the covalent docking study of **2.** As shown in Figure 2, the binding mode of **2** in the ATP-binding cleft was very similar to that of **1**, except that the additional acryl group of **2** formed a covalent bond with the SH group of Cys797.[34] A hydrogen bond was also formed between the

pyrimidine N1 and Met793 in the kinase hinge region. The hydroxyl group of (*S*)-2-phenylglycinol formed an additional H-bond with Asp855. Moreover, the furanopyrimidine core and the three phenyl moieties made close contact as sigma-pi hydrophobic interactions with the residues of Val726, Ala743, Lys745, Leu788, Leu718, and Thr790. The above analysis indicated that the structure-activity relationship (SAR) studies should focus on the 5,6-fused pyrimidine (hinge binding) and the perpendicular phenyl ring with the Michael acceptor group (covalent binding), and also explore possible modification sites to expand the structural diversity and identify the most promising drug candidate.

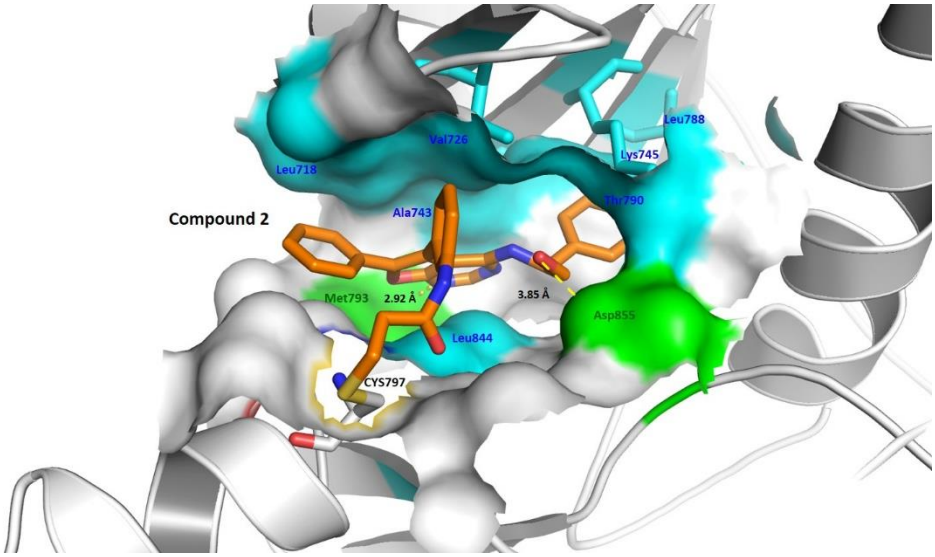

Figure 2. The binding site analysis for compound **2** (orange) docking with EGFR X-ray protein (PDB code: 4JQ7). Compound **2** forms a covalent bond with Cys797 (as shown in white color residue), and hydrogen bond with Met793 (as shown in green color residue). The hydrophobic effect was contributed by Leu718, Val726, Ala743, Lys745, Leu788, and Leu844 (as shown in cyan color residues).

Chemistry

Compounds **42**–**48** were synthesized as illustrated in Schemes 1 and 2. We synthesized the building blocks **7**, **10**, **13,** and **17** from appropriate nitrobenzene derivatives (**5**, **8**, **11**, and **14**) through modification of published procedures or known methods.[35–39] In short, the cyclization of the 2-hydroxy-1-(3-nitrophenyl)-1-ethanone (**6**) or *N*-hydroxy-3-nitrobenzimidoyl chloride (**16**) with malononitrile under basic conditions yielded the furan **7** and the isoxazole **17**, respectively. The nitrobenzene derivatives **8** and **11** were individually condensed with ethyl cyanoacetate and malononitrile followed by cyclization in the presence of octasulfur to obtain the thiophenes **10** and **13**.[40] The required five-membered heteroaryl compounds **7**, **10**, **13**, and **17** were cyclized and then chlorinated to synthesize the bicyclic [2,3-*d*]pyrimidines **22**–**26**, as shown in Scheme 2. The nucleophilic aromatic substitution with (*S*)-(+)-2-phenylglycinol derivatives gave the desired compounds **29**–**35**. Bromo-substituent **30** was cross-coupled with methyl zinc chloride using Negishi coupling to prepare the methylated compound **31**. The reduction of **29**–**35** using 10% Pd/C in presence of hydrogen gas, iron powder under acidic condition, or stannic chloride yielded the corresponding amino analogues **36**–**41**. Amide bond formation of compounds **36**–**41** with acrylic acid was accomplished in presence of 1-(3-dimethylaminopropyl)-3-ethylcarbodiimide hydrochloride (EDCI·HCl) to obtain the corresponding acrylamides **42, 43**, and **45**–**47**. The desilylation of OTBS-protected **47** was carried out with tetrabutylammonium fluoride (TBAF) to give the desired isoxazolo[5,4-

d]pyrimidine **48**. On the other hand, acrylation of the aniline **38** using acryloyl chloride led to the acrylamide **44**. The synthetic routes for the preparation of amide **70**–**85** are outlined in Scheme 3, considering various functional groups attached to the terminal end of the Michael acceptor. Starting compounds **49**–**51** were synthesized by modifying reported procedures.[36,41] Bromination of the furan and the thiophene rings at 3-position with *N*-bromosuccinimide (NBS) followed by nucleophilic substitution by (*R*)-(+)-1-phenylethylamine, (*R*)-(−)- or (*S*)-(+)-2-phenylglycinol led to analogues **55**–**59**. Suzuki cross-coupling of analogues **55**–**59** with 3-nitrophenylboronic acid yielded the nitro analogues **60**–**64**. Similarly to the synthesis of **42**–**48**, aniline compounds **65**–**69** were obtained by reduction of the corresponding nitro compounds **60**–**64** and subsequent coupling with various carboxylic acids or 2-chloroethanesulfonyl chloride to obtain the analogues **70**–**85**.

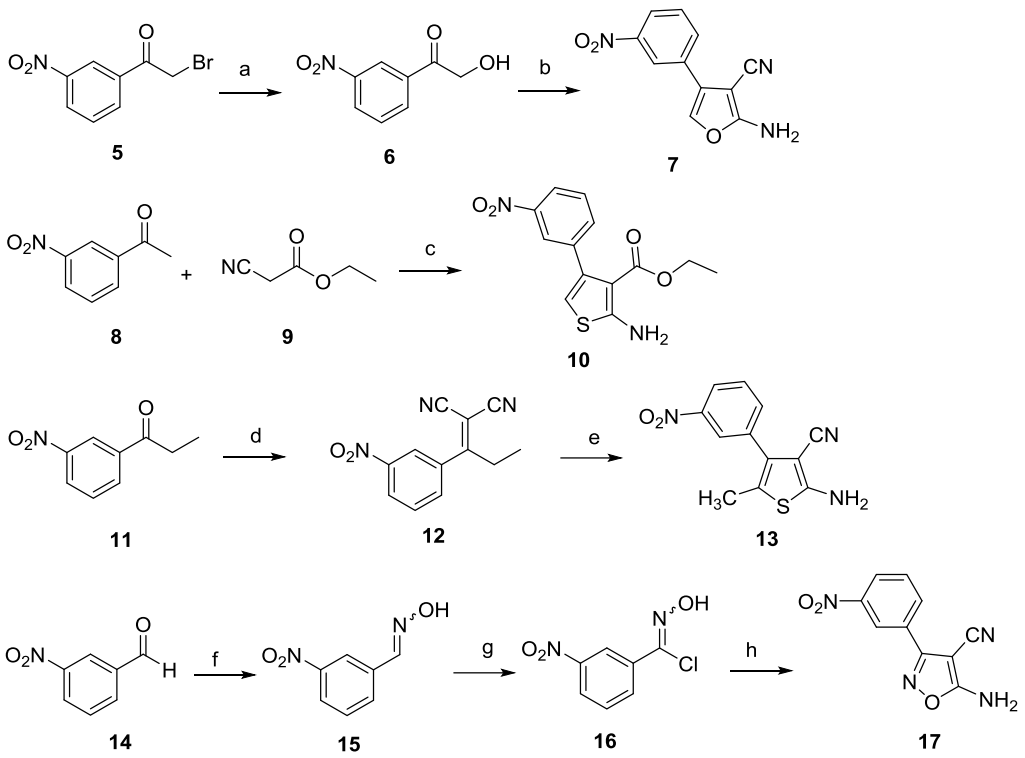

[a]Reagents and conditions: (a) $AgNO_3$, H_2O, acetone, reflux, 68%; (b) malononitrile, Et_2NH, DMF, r.t., 52%; (c) morpholine, S_8, ethanol, 60 °C, 43%; (d) malononitrile, NH_4OAc, acetic acid, benzene, reflux, 71%; (e) S_8, Et_2NH, ethanol, reflux, 83%; (f) $NH_2OH_{(aq)}$, ethanol, r.t.; (g) NCS, DMF, r.t.; (h) NaOEt, malononitrile, r.t. to 45 °C, 51%

Scheme 1. Synthesis of the building blocks **7**, **10**, **13**, and **17**.[a]

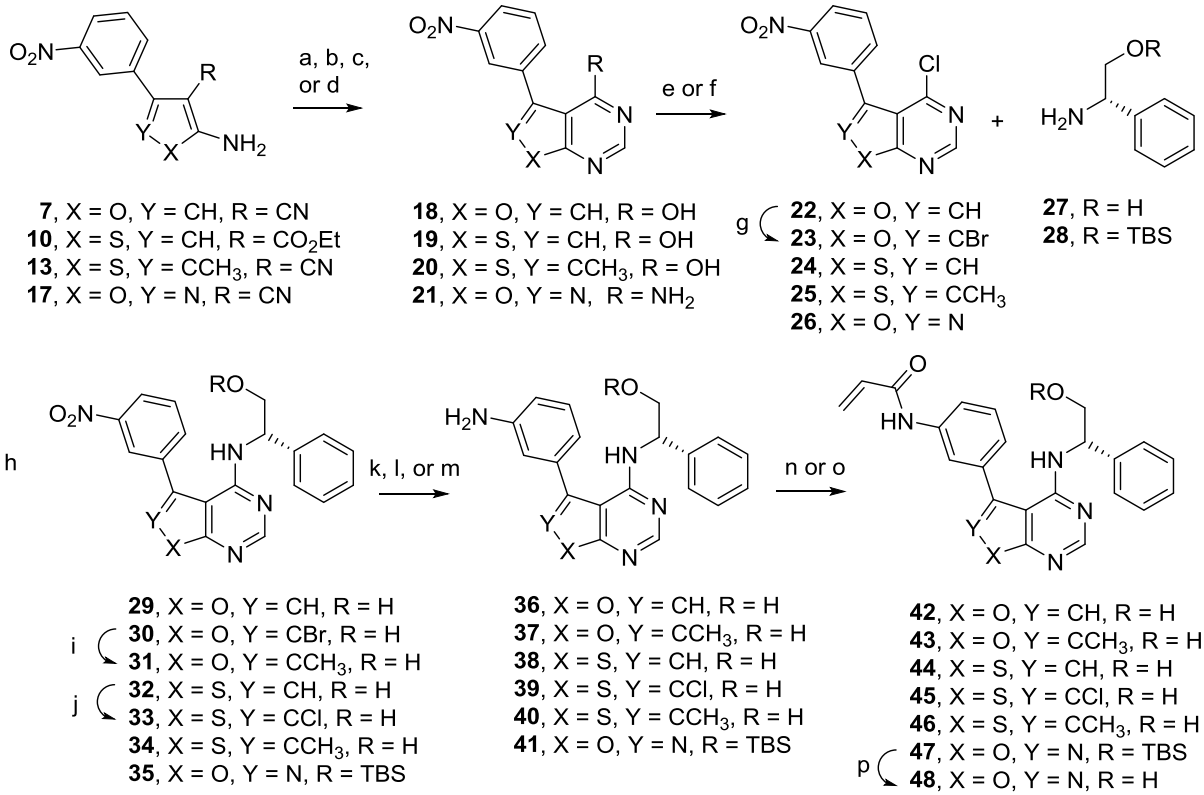

[a]Reagents and conditions: (a) Ac_2O, HCO_2H, 100 °C; (b) $HCONH_2$, 200 °C; (c) HCO_2H, H_2SO_4, microwave; (d) i. $HC(OEt)_3$, toluene, 150 °C; ii. NH_3 in methanol, ethanol, r.t.; (e) $POCl_3$, heat; (f) *tert*-butyl nitrile, TMSCl, DMF, r.t.; (g) NBS, DMF, r.t.; (h) Et_3N, ethanol, reflux; (i) $Pd(PPh_3)_4$, MeZnCl, THF, 80 °C; (j) NCS, DMF, r.t.; (k) $SnCl_2$, ethanol, reflux; (l) H_2, Pd/C; (m) iron powder, acid condition, ethanol, heat; (n) acrylic acid, EDCI; (o) acryloyl chloride, pyridine, r.t.; (p) TBAF, THF, r.t.

Scheme 2. Synthetic route of the EGFR inhibitors for simplification and replacement of furanopyrimidine through scaffold-hopping.[a]

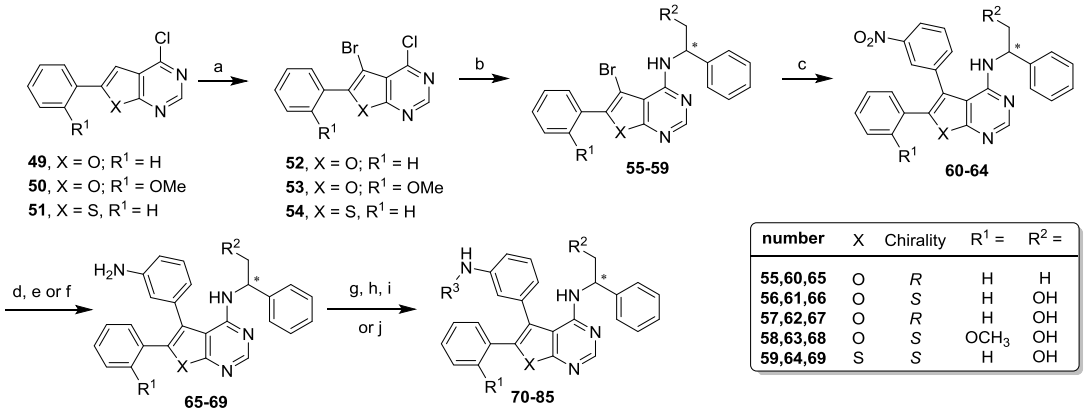

number	X	Chirality	R^1 =	R^2 =
55,60,65	O	*R*	H	H
56,61,66	O	*S*	H	OH
57,62,67	O	*R*	H	OH
58,63,68	O	*S*	OCH_3	OH
59,64,69	S	*S*	H	OH

number	X	Chirality	R^1 =	R^2 =	R^3 =
70	O	*R*	H	H	acryloyl
71	O	*S*	H	OH	but-2-ynoyl
72	O	*S*	H	OH	vinylsulfonyl
73	O	*S*	H	OH	(*E*)-but-2-enoyl
74	O	*S*	H	OH	(*E*)-5-methylhex-2-enoyl
75	O	*S*	H	OH	(*E*)-cinnamoyl
76	O	*S*	H	OH	(*E*)-3-carboxyacryl
77	O	*S*	H	OH	(*E*)-4-ethoxy-4-oxobut-2-enoyl
78	O	*S*	H	OH	(*E*)-4-(dimethylamino)but-2-enoyl
79	O	*S*	H	OH	(*E*)-4-(diethylamino)but-2-enoyl
80	O	*S*	H	OH	(*E*)-(4-(ethyl(2-hydroxyethyl)amino)but-2-enoyl
81	O	*S*	H	OH	(*E*)-*N*-(4-morpholinobut-2-enoyl
82	O	*S*	OCH_3	OH	acryloyl
83	O	*R*	H	OH	acryloyl
84	O	*R*	H	OH	(*E*)-4-(dimethylamino)but-2-enoyl
85	S	*S*	H	OH	acryloyl

[a]Reagents and conditions: (a) NBS, DMF; (b) **27** or (*R*)-(-)-2-phenylglycinol, Et_3N, ethanol, heat; (c) $Pd(dppf)_2Cl_2$, 3-nitrophenylboronic acid, $Na_2CO_{3(aq)}$, heat; (d) $SnCl_2$, ethanol, reflux; (e) H_2, Pd/C; (f) iron powder, acetic acid, ethanol, 90 °C; (g) acryloyl chloride, pyridine, r.t.; (h) acrylic acid, EDCI; (i) 2-chloroethanesulfonyl chloride, Et_3N, CH_2Cl_2; (j) i. 4-bromocrotonoic acid, EDCI-HCl; ii. various amine

Scheme 3. Synthesis of EGFR inhibitors with various Michael acceptors.[a]

Biological Evaluation of EGFR Activating Mutations and SAR Analysis

All the novel synthesized compounds were evaluated by $EGFR^{WT}$, $EGFR^{L858R/T790M}$ kinase assays, as well as on two NSCLC cell lines: HCC827[28] (expressing $EGFR^{del19}$) and H1975 (expressing $EGFR^{L858/T790M}$). The biological data are shown in Tables 1 and 2. Compound **2** was used as the starting point for the structure-activity and lead optimization studies.

In order to understand how the EGFR inhibitory activity was affected by the compound structure, a preliminary SAR study was performed. Removal of the hydroxyl group from the 2-phenylglycinol fragment of **2** significantly decreased $EGFR^{WT}$ and $EGFR^{L858R/T790M}$ activity by

over 6-fold and 18-fold, respectively (*cf.* **2** *versus* **70**). This result is in good agreement with our SBDD analysis and indicates that the hydroxyl group (forming a H-bond with Asp855) plays an important role in maintaining a potent activity against both wild-type and double mutant EGFR kinases.

Replacement of the phenyl group in the 6-position of the furanopyrimidine scaffold with H and Me led to a significantly reduced inhibition of $EGFR^{WT}$ and $EGFR^{L858R/T790M}$ (*cf.* **2** *versus* **42** and **43**). These results indicate that the sigma-pi interactions formed by the phenyl group at the 6-position are essential for EGFR inhibition, especially of $EGFR^{L858R/T790M}$. Compounds **2** and **42** were then used by docking method to illustrate the binding interaction in EGFR double mutations X-ray structure (PDBID: 5CAS). As shown in Figure 3A, the binding mode of compound **42** was twisted and induced a steric clash with Met790 as well as influenced on the Michael acceptor's binding, which is a crucial factor that compound **42** lost the activity of $EGFR^{L858R/T790M}$. Furthermore, the introduction of the *ortho*-methoxy group on the 6-phenyl moiety caused a 6-fold loss of $EGFR^{L858R/T790M}$ inhibitory activity likely because of the steric hindrance between two phenyl rings at 5- and 6-position. It can be concluded from these observations that the 6-phenyl ring lies perpendicular to the 5-phenyl and that the right positioning of the acrylamide relative to the thiol of Cys797 is crucial for covalent bond formation. High $EGFR^{L858R/T790M}$ inhibition activity can be achieved when the acrylamide moiety points to the Cys797 in the protein binding pocket.

Furthermore, we conducted a scaffold-hopping strategy by replacing the furanopyrimidine with thieno[2,3-*d*]pyrimidine and isoxazolo[5,4-*d*]pyrimidine to obtain **44**–**46**, **48**, and **85**. Although these compounds maintained submicromolar IC_{50} and CC_{50} against $EGFR^{WT}$ kinase inhibition and HCC827 cell proliferation, their inhibitory activity for $EGFR^{L858R/T790M}$ was greatly reduced (**44**–**46**, **48**, and **85**; $EGFR^{L858R/T790M}$ IC_{50} = 650–4626 nM). It is thus concluded that furanopyrimidine along with two phenyl rings at 5 and 6-positions is a promising scaffold on which to conduct further SAR studies in order to identify potential EGFR clinical candidates.

Table 1. SAR investigation by scaffold modifications[a].

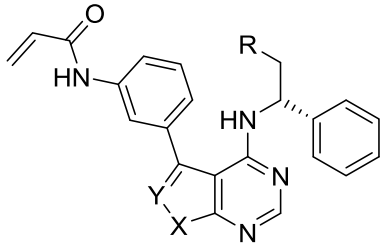

Compound No.	X	Y	R	$EGFR^{WT}$ IC_{50} (nM)[b]	$EGFR^{L858R/T790M}$ IC_{50} (nM)[b]	HCC827 CC_{50} (nM)[c]	H1975 CC_{50} (nM)[c]
2	O	CPh	OH	20±10	27±10	24±11	1,258±302
70	O	CPh	H	117	500	58	4300
42	O	CH	OH	159±65	>10,000	744±197	>20,000
43	O	CCH_3	OH	62±22	1,322±487	46±5	>20,000
82	O	C-2'OMePh	OH	24±10	157±54	34±4	4,076±1,600
44	S	CH	OH	82±44	2,316±819	56±21	>20,000
45	S	CCl	OH	81±36	1,080±365	51±11	8,656±4,490
46	S	CCH_3	OH	107±35	1,259±201	35±13	12,564±5,945
85	S	CPh	OH	136±36	650±209	146±32	10,721±1,267
48	O	N	OH	416±244	4,626±2,359	105±16	>20,000
gefitinib	–	–	–	29±13	6,746±1,205	26±6	18,755±2,778
afatinib	–	–	–	14±6	22±7	14±4	224±58

[a]IC_{50} and CC_{50} data are expressed as the mean of at least three independent determinations, presented as mean±SD; [b]The IC_{50} value was defined as the amount of compound that induced a 50% inhibition in enzyme activity in comparison with DMSO-treated controls; [c]The CC_{50} value was defined as the amount of compound that caused 50% reduction in cell viability in comparison with DMSO-treated controls.

Table 2. SAR investigation of Michael acceptors and side chain chirality[a].

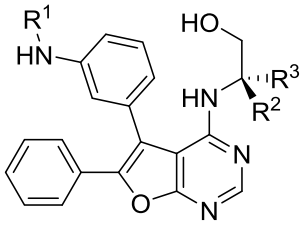

Compound	R^1	R^2	R^3	$EGFR^{WT}$ IC_{50} (nM)[b]	$EGFR^{L858R/T790M}$ IC_{50} (nM)[b]	HCC827 CC_{50} (nM)[c]	H1975 CC_{50} (nM)[c]
1	–	H	Ph	223	>10000	518	ND
2		H	Ph	20±10	27±10	24±11	1258±302
71	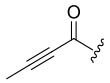	H	Ph	64±22	6,370±2,043	182±16	6,740±4,429
72		H	Ph	3,675±1,196	2,459±987	2,707±127	7,243±2,813
73	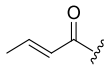	H	Ph	239±49	>10,000	307±130	13,211±2,450
74	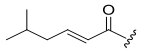	H	Ph	>10,000	>10,000	679±28	>20,000
75	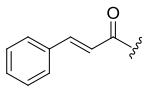	H	Ph	5,004±1,687	>10,000	1,780±93	>20,000
76	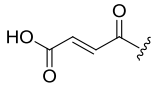	H	Ph	3,059±941	>10,000	4,116±499	>20,000
77	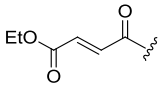	H	Ph	79±33	779±157	516±210	7,007±3,715
78	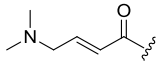	H	Ph	15±5	48±12	25±8	620±104

79	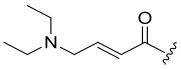	H	Ph	14±5	131±24	62±7	2,482±417
80	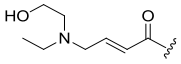	H	Ph	13±2	117±40	19±5	2,413±787
81	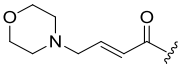	H	Ph	19±7	283±34	17±7	2,830±1,503
83		Ph	H	238±38	147±39	840±78	13,397±2.310
84	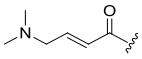	Ph	H	562±37	1,061±59	1,046±35	6,943±1.166
gefitinib	-	-	-	29±13	6,746±1,205	26±6	18,755±2,778
afatinib	-	-	-	14±6	22±7	14±4	224±58

[a]IC_{50} and CC_{50} data are expressed as the mean of at least three independent determinations, presented as mean ± SD; [b]The IC_{50} value was defined as the amount of compound that induced a 50% inhibition in enzyme activity in comparison with DMSO-treated controls; [c]The CC_{50} value was defined as the amount of compound that caused 50% reduction in cell viability in comparison with DMSO-treated controls.

Next, we explored the possibility of attaching a variety of Michael acceptors to the 5-phenyl group of the furanopyrimidine core (Table 2). At first, we attempted to replace the acrylamide group with butynamide and vinyl sulfonamide. The butynamide **71** inhibited EGFR in a concentration range very similar to that of gefitinib, while the vinyl sulfonamide **72** drastically reduced the kinases activities of wild-type and double mutant. Acrylamide group was thus concluded to be an appropriate Michael acceptor to have in the optimized molecule.

A series of functional groups were introduced into C=C in order to improve cellular activity, including hydrophobic groups (alkyl and phenyl groups) and hydrophilic groups (acid, ester, amine, and alcohol). Molecule extension with various hydrophobic groups at the terminal double bond resulted in a loss of potency against wild-type and double mutant kinases, respectively (*cf.* **2** *versus* **73**–**75**). To explain the poor activities of compounds **73**–**76** we applied covalent docking strategy for compound **74** with the EGFR wild type X-ray (PDB code: 4JQ7) and double mutation X-ray (PDB code: 5CAS) as representatives. In both of binding mode analysis, the isopropyl group in terminal double bond of compound **74** has a steric clash with the Asp800 of wild-type and double mutation proteins, that may give an explanation why introduction of hydrophobic alkyl or phenyl group lost their inhibition activities (Figures 3B and 3D). While attachment of carboxylic acid ethyl ester to Michael acceptor led to compound **77** displayed moderate inhibition in EGFR assays. According to its binding modes with $EGFR^{WT}$ and $EGFR^{L858R/T790M}$, the ethyl ester group of **77** evaded a steric clash from Asp800. (Figure 3C and 3E). In T790M and L858R mutation proteins, the modeling exhibited an extra strong hydrogen bond interaction with the Cys797 backbone NH and two hydrogen bonds with Asn842 and Arg855 (Figure 3E). By contrast, introduction of $–CO_2H$ lost its bioactivities due to electronic repulsion with $–CO_2H$ of Asp800. (*i.e.,* **76**). Moreover, extension with di-substituted amino groups at the terminal double bond (*i.e.,* **78**–**81**) maintained EGFR activities (*i.e.,* **78**–**81**). It is noteworthy that di-substituted amino functionalities are well tolerated for the

activity against HCC827 cells (**78**–**81**, CC_{50} = 17–62 nM). When the size of the alkyl substituent of amino group increased, inhibition of $EGFR^{L858R/T790M}$ slightly decreased (*cf.* **78** *versus* **79**–**81**), but inhibition of $EGFR^{WT}$ remained comparable to that by lead compound **2**. Based on the X-ray structure of EGFR proteins, Asp800 is adjacent to Cys797 in the binding pocket.[42] Incorporating a nitrogen containing a basic group onto the acrylamide β-position may form a plausible ionic interaction between the protonated nitrogen of amino side chain and the acid residue of Asp800, which improved the recognition of compound **78**–**81** in the active site.[42,43] It may also assist the nucleophilic attack at the Michael acceptor by Cys797.[43] Among all the new EGFR inhibitors synthesized, dimethylamino compound **78** showed the highest inhibitory activity against HCC827 (CC_{50} = 25 nM) and H1975 (CC_{50} = 620 nM) cell lines. In addition, (*R*)-enantiomers **83** and **84** led to over 5-fold lower kinase activity and 10-fold anti-proliferative activity compared to the corresponding (*S*)-isomers (*cf.* **2** *versus* **83** and **78** *versus* **84**), respectively (Table 2). These results indicated that the (*S*) configuration of 2-phenylglycinol side chain is essential for the EGFR activities. Compound **78** with an acrylamide moiety possess irreversible kinase inhibitor character, which showed potent activity against $EGFR^{L858R/T790M}$ similar to afatinib. However, further toxicity study and antitumor efficacy of **78** in *in vivo* experiments are evaluated in following section.

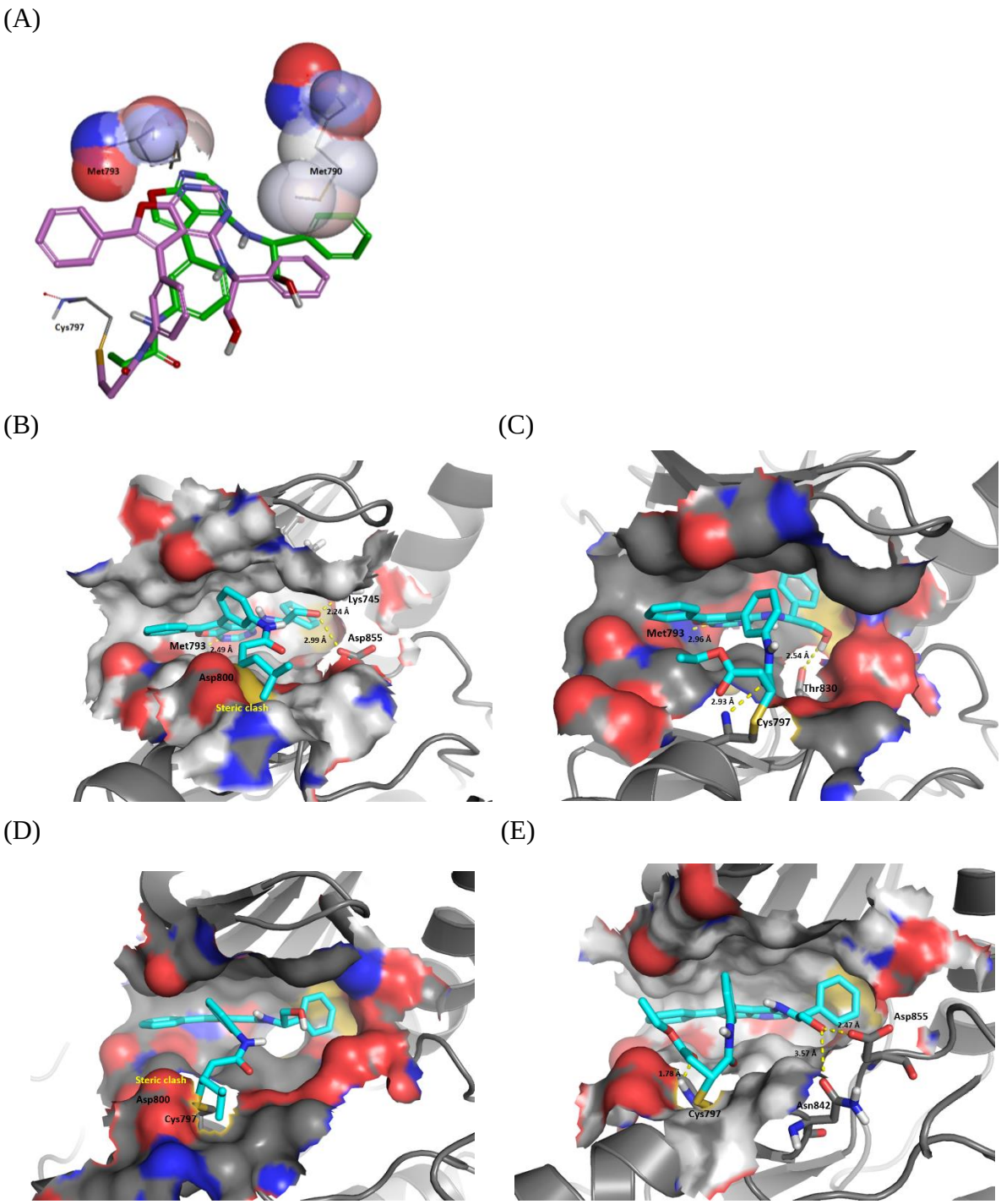

Figure 3. Characterization of inhibitor binding modes: (A) the binding mode of compound **2** (pink) overlaid with **42** (green) in $EGFR^{L858R/T790M}$ protein (PDB code: 5CAS); (B) $EGFR^{WT}$ protein−inhibitor interactions for compound **74** (PDB code: 4JQ7); (C) $EGFR^{WT}$ protein−inhibitor interactions for compound **77** (PDB code: 4JQ7); (D) $EGFR^{L858R/T790M}$

protein−inhibitor interactions for compound **74** (PDB code: 5CAS); (E) $EGFR^{L858R/T790M}$ protein−inhibitor interactions for compound **77** (PDB code: 5CAS).

Biological Evaluation of EGFR and HER2 Exon 20 Insertion Mutations.

Amino acids deletions of exon 19 and the exon 21 L858R point mutation are most common EGFR mutations and considered as the classic activating mutations in NSCLC.[44] Patients with classic mutations are highly response to first and second-line standard EGFR TKIs therapy, including erlotinib, gefitinib, afatinib and osimertinib.[44] Highly heterogeneous exon 20 insertions are the third most prevalent non-classic EGFR activating mutations and accounted for approximately 4–10% of all EGFR mutations.[45] Response rates of patients with exon 20 insertions to standard EGFR targeted therapy are generally poor compared with classic mutations.[45–47] Oncogenic function of HER2 mutations and overexpression play an important role in various cancer types. In particular, HER2 exon 20 insertions are found in 1–3% of NSCLC patients.[48] Currently no EGFR- or HER2-directed therapies are approved specifically for the treatment of both mutations. Two investigational drugs, poziotinib and TAK-788, are undergoing phase II (NCT03066206) and phase I/II clinical trial (NCT02716116), respectively.[49,50] Recent trial data displayed that poziotinib achieved 64% of objective response rate (ORR) in EGFR and HER2 exon 20 mutant NSCLC (NCT03066206).[51,52] Herein, we selected four compounds (**70**, **78**, **82**, **85**) to examine their inhibitory activities against three

types of EGFR and one type of HER2 exon 20 insertions enzymatic assays along with pozitotinib and osimertinib as references. Those compounds were also evaluated for their inhibitory activity in A431 cell line (expressing $EGFR^{WT}$). As seen in Table 3, among of three furanopyrimidines (**70**, **78**, **82**), **78** exhibited equal potency compared with poziotinib and 7−25 folds more potent than osimertinib in both EGFR and HER2 exon 20 insertion assays.[53] Moreover, **78** showed 33-fold weaker inhibition than poziotinib against A431 cells and similar inhibition to osimertinib that spare wild-type EGFR. The results indicated that **78** exhibited potentially higher therapeutic window than poziotinib. Furanopyrimidines **70** and **82** possessed moderate activities against three EGFR exon 20 insertion enzymes, but almost lost activity against HER2 exon 20 insertion enzyme. More interestingly, thienopyrimidine **85** dramatically decreased its inhibition in both exon 20 insertion assays, which indicated oxygen-containing scaffold **78** is much tighter binding to exon 20 insertion enzymes than thiol-containing scaffold **85**.

Table 3. Inhibition of EGFR and HER2 exon 20 insertions assays and A431 cellular assay.[a,b]

Compound	EGFR exon 20 insertions IC_{50} (nM)[a]			HER2 exon 20 insertion IC_{50} (nM)[a]	A431 CC_{50} (nM)[b]
	$EGFR^{A763\_Y764insFHEA}$	$EGFR^{D770GY}$	$EGFR^{D770\_N771insNPG}$	$HER2^{V777\_G778insCG}$	
70	0.214	0.641	1.48	8.13	449
78	0.043	0.033	0.133	0.203	1020
82	0.145	0.295	0.636	5.20	>8,010

85	1.15	4.82	17.8	369	>20,000
Poziotinib	0.078	0.082	0.218	0.206	31
Osimertinib	0.421	0.858	0.950	3.31	967

[a]The IC_{50} value was defined as the amount of compound that induced a 50% inhibition in enzyme activity in comparison with DMSO-treated controls; Compounds were tested in 10-dose IC_{50} mode with 4-fold serial dilution starting at 5 μM. And control compound, staurosporine, was tested in 10-dose IC_{50} mode with 4-fold serial dilution starting at 20 μM. [b]In cell-based assay, compounds were tested in 9-dose CC_{50} mode with 4-fold serial dilution starting at 20 μM.; The CC_{50} data are expressed as the mean of at least three independent determinations.

X-ray Co-crystal Study of Wild-Type EGFR Kinase in Complex with 78

EGFR crystals were soaked in compound **78** and the resulting EGFR/**78** complex crystal structure was resolved to 2.86Å. The electron density map clearly showed that **78** formed a covalent bond with Cys797 in the ATP-binding site through the Michael acceptor (enone) (Figure 4). The (*S*)-2-phenylglycinol fragment of **78** occupied the region around the gatekeeper and formed hydrophobic interactions with Thr790, Lys745, and Met766 (Figure 4). The hydroxyl group of **78** formed hydrogen bonds with Asp855 on the DFG motif. The pyrimidine core structure aligned with the hinge region and formed hydrophobic interactions with Leu718 in the starting site of P-loop and also with Ala743, Thr790, and Leu844. Two separated phenyl

rings extended from the furanopyrimidine core perpendicular to each other. The 6-phenyl group on the same plane as the pyrimidine core formed hydrophobic interactions with Leu844, while the perpendicular 5-phenyl ring formed hydrophobic interactions with Val726 on the β-sheet. The Michael acceptor linked to this perpendicular 5-phenyl ring formed the important covalent bond with residue Cys797. This Michael addition was close to the acidic residue Asp800. Moreover, the conserved DFG motif and His-Arg-Asp (HRD) triad motif of protein kinase play a major role in the regulation of kinase activity.[54–56] In EGFR/**78** complex crystal structure, a unique hydrogen bond network was observed between the hydroxyl group of the (*S*)-2-phenylglycinol fragment of **78** and the DFG and HRD motifs in the activation loop of EGFR (Figure 5). The hydroxyl group formed hydrogen bonds with Asp855 of the DFG motif and to the HRD motif via Asp855 and Asn842. While the hydrogen bond interactions are absent by removed hydroxyl group from (*S*)-2-phenylglycinol moiety, the inhibitory activity decreased significantly (*cf.* **70** *versus* **78** and **2**). The hydrogen bond network interactions between **78** and the DFG and HRD motif greatly contribute to its potency. Altogether, compound **78** occupied the ATP-binding site and interacts with surrounding residues by covalent bonding, hydrogen bonds, and hydrophobic interactions, which gave it a potent inhibitory activity against wild-type EGFR.

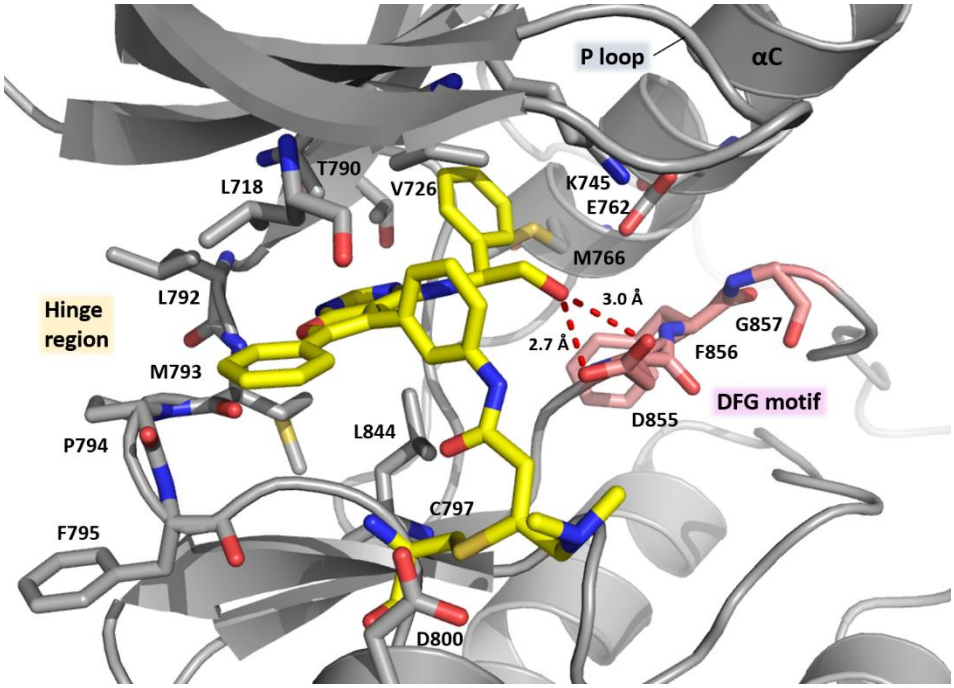

Figure 4. Crystal structure of EGFR in complex with **78** (yellow). For clarity, M766 (on αC helix) and P-loop were omitted in the figure (PDB code: 6JZ0).

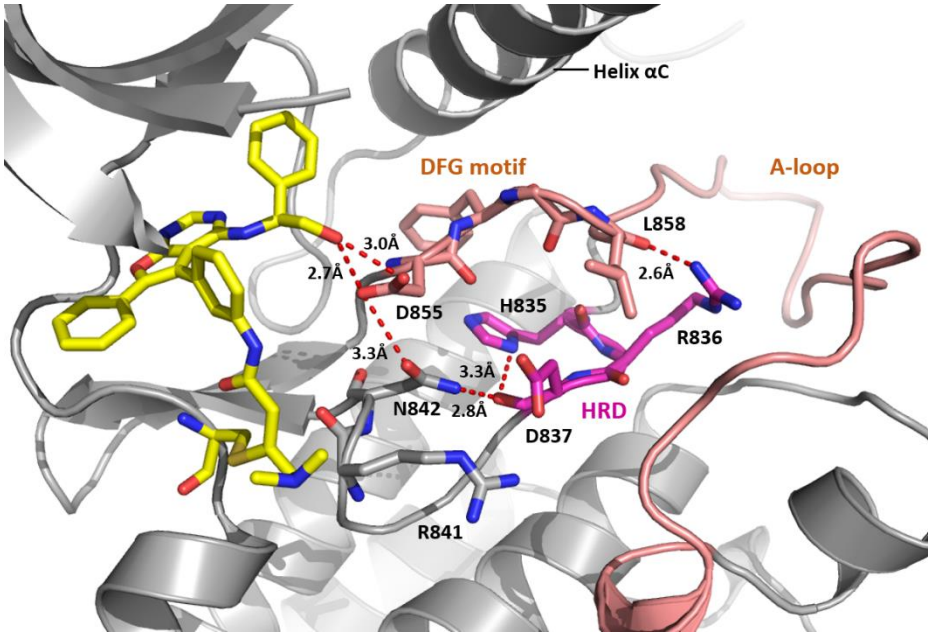

Figure 5. Compound **78** (yellow) forms a hydrogen bond network with the DFG (pink) and HRD motifs (magenta) in the activation loop through the hydroxyl group of the (*S*)-2-

phenylglycinol fragment. The distances between **78** and EGFR kinase domain were labeled (PDB code: 6JZ0).

Pharmacokinetic Study

We carried out pharmacokinetic (PK) evaluations of compounds **2** and **78** in rats. We found that **78** showed a much better PK profile than compound **2** (Table 4). Moreover, when administered by IV injection, **78** exhibited a lower clearance and volume distribution, as well as 50% higher AUC than the approved irreversible-binding drug, afatinib. When administered orally (P.O.), **78** displayed an approximately 4-fold higher AUC than afatinib and around 41.5% oral bioavailability.

Table 4. Pharmacokinetics Profile of compound **2**, **78**, and afatinib in rat.

	I.V. (5 mg/kg)				P.O. (20 mg/kg)				
Compound	**$t_{1/2}$ (h)**	**CL (ml/min/kg)**	**V_{ss} (l/kg)**	**$AUC_{(0\text{-inf})}$ (ng/mL*h)**	**$t_{1/2}$ (h)**	**C_{max} (ng/mL)**	**T_{max} (h)**	**$AUC_{(0\text{-inf})}$ (ng/mL*h)**	**F (%)**
2	0.5	76.5	2.3	1096	0.9	193	1.2	303	5.5
78[a]	2.3	55.6	8.6	1520	3.4	508	3.3	2978	41.5
afatinib	5.7	79.2	28.7	1063	6	75.2	4.2	676	15.9

[a]5 mg/kg for I.V. injection and 23.6 mg/kg for P.O. administration

Western Blotting Analysis

In order to probe the full potential of **78**, we evaluated its ability to interfere with EGFR signaling inside the cell by western blotting. To this end, HCC827 and H1975 cells were treated

with different doses of **78** and then were analyzed for EGFR autophosphorylation (pEGFR at residue Tyr1068). As shown in Figure 6A, **78** showed a similar inhibitory level of EGFR autophosphorylation compared to gefitinib in HCC827 cells. In Figure 6B, it is observed that **78** induced reduction of phosphorylated EGFR in a dose-dependent manner in H1975 cells. The western blotting results were consistent with two cell-based growth inhibition data, which are showed in Table 2.

(A)

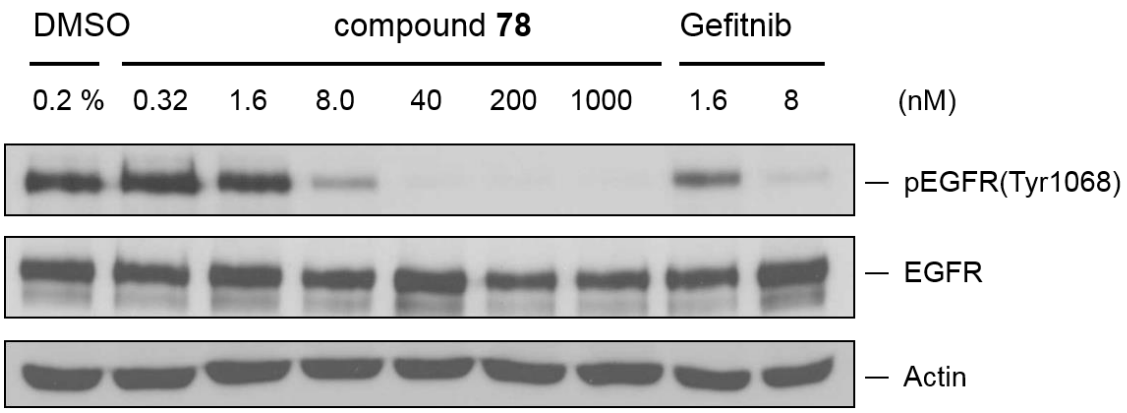

(B)

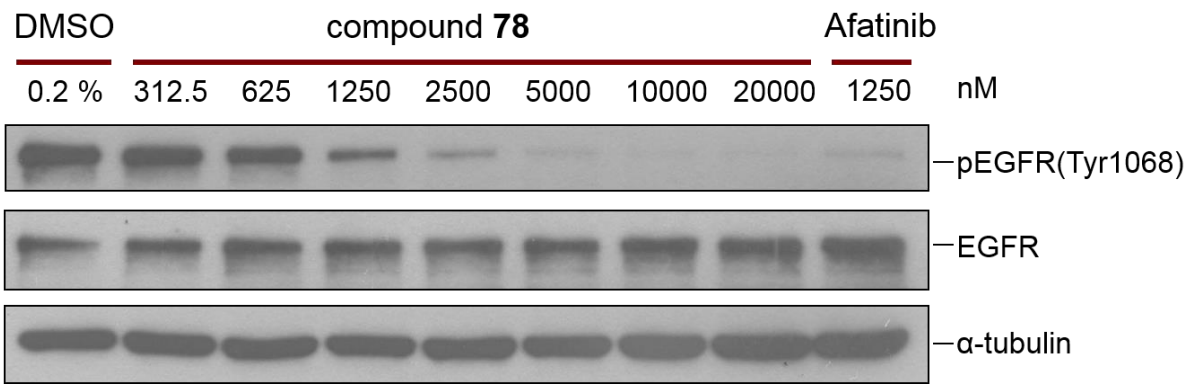

Figure 6. Western blot analysis: (A) By using anti-phospho-EGFR Y1068 and anti-EGFR

immunoblots of HCC827 cell lysates treated with **78** and gefitinib; (B) By using anti-phospho-EGFR Y1068 and anti-EGFR immunoblots of H1975 cell lysates treated with **78** and afatinib.

Kinase Profiling

To examine the specificity of the highly promising compound **78**, we subjected it to kinase profiling using the KINOME*scan* technology against a panel of 456 kinases (containing 395 non-mutant kinases) at a concentration of 10,000 nM (Figure 7). $EGFR^{WT}$ and all EGFR mutants were potently inhibited by **78** (0–7.6% of control value at 10,000 nM). Due to the irreversible inhibition it causes, **78** also exhibited high affinity against kinases bearing a cysteine structurally analogous to Cys797 in EGFR, such as BLK (0.25%), BMX (4.8%), BTK (3%), ERBB2 (0%), ERBB4 (0.05%), JAK3 (0%), and TEC (5.6%). Moreover, other off-target kinases showing apparent binding included LOK, SLK, and TXK (<10% of control value). The selectivity score is a quantitative measure of compound selectivity and it is defined as S(10) = (number of non-mutant kinases with <10% control value inhibition)/(number of non-mutant kinases tested). The S(10) selectivity score, calculated using <10% of control as potency threshold at a concentration of 10,000 nM, was determined to be 0.028 (11/395). These results overall indicated that **78** has a high selectivity and low off-target effects, suggesting a safety index suitable for further development.

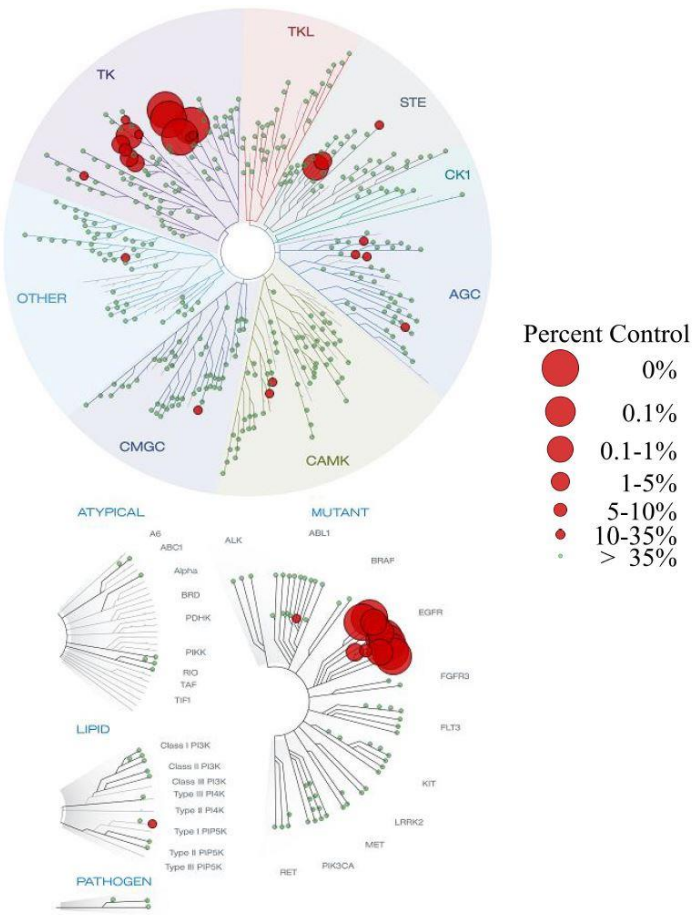

Figure 7. Kinase profiling of **78** using the KINOMEScan technology.

Toxicity and Efficacy *In Vivo* of Compound 78

First of all, we evaluated acute toxicity of **78** by orally treating **78** into ICR mice at a dose of 100 mg/kg once a day (QD) for two weeks. Afatinib (100 mg/kg) was also examined at the same dosing schedule for comparison. Mice treated with afatinib were observed severe fur loss in the nose and abdomen and skin rash, but no apparent changes were observed for the group treated with **78**. It is indicated that furanopyrimidine **78** possessed lower off-target effects and higher dose tolerance than afatinib.

The compound profile of **78** encouraged us to assess its *in vivo* anticancer activity in EGFR mutant NSCLC models. HCC827 and H1975 xenograft models were developed by inoculating nude mice subcutaneously with the corresponding cancer cells. In the HCC827 tumor model, mice were treated with oral administration of **78** for 5 days/week for 2 consecutive weeks (days 1–5 and 8–12). At dosages of 20 and 50 mg/kg of **78**, tumor growth was significantly reduced ($p<0.05$), demonstrating the potent *in vivo* anticancer activity of **78** (Figure 8). No significant differences in body weight change or other adverse effects were observed upon treatment with compound **78**. Administration of the reference compound gefitinib (20 mg/kg) and afatinib (20 mg/kg) by perioral route using the same schedule also shrank the tumor significantly ($p<0.05$). Approximately 5% body weight loss was observed in afatinib-treated mice.

(A) (B)

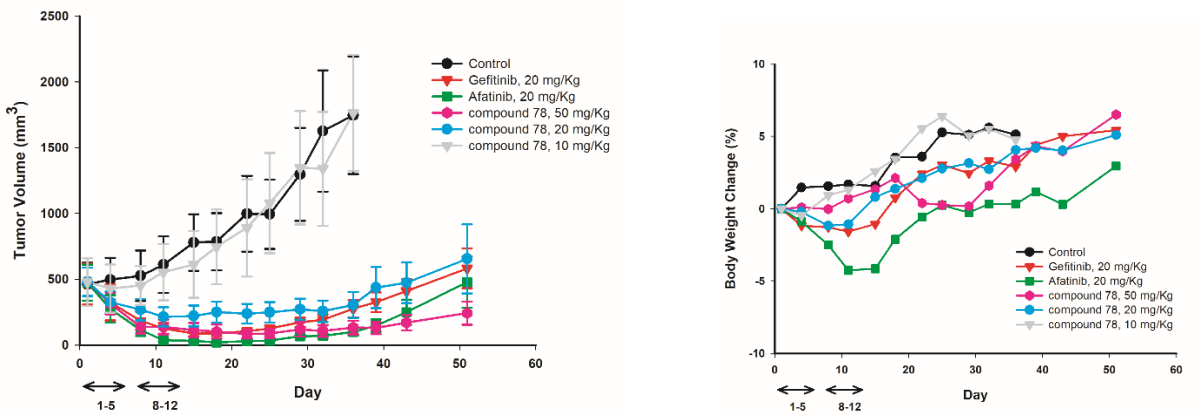

Figure 8. (A) *In vivo* antitumor efficacy of gefitinib, afatinib, and **78** in HCC827 xenograft mouse model. (B) Body weight change (%) of the mice in HCC827 xenograft mouse model.

In the H1975 tumor model, the *in vivo* efficacy was evaluated through oral administration of afatinib (15 mg/kg) and **78** (50 mg/kg) QD for 15 days, respectively. The mean tumor size of the vehicle control group reached 2044 mm^3 on day 22 after tumor inoculation. Treatment with afatinib at 15 mg/kg had a significant antitumor effect compared with the control group, suppressing tumor growth by 65%. Treatment with **78** only at 50 mg/kg also had a significant antitumor effect (mean tumor growth inhibition of 34%, range: 22–48%). The test compound **78** and afatinib were tolerated well by the tumor-bearing mice at 50 mg/kg and 15 mg/kg, respectively, and no severe body weight loss was observed during the studies.

Table 5. Antitumor activity of **78** and afatinib as a single agent in the treatment of subcutaneous H1975 human lung cancer xenograft model.

Treatment	**Tumor Size (mm^3)**[a]	**Tumor growth inhibition (TGI, %)**	***p*-value**[b]
Vehicle	2044±161	—	—
Afatinib (15 mg/kg)	706±92	65	<0.001
78 (50 mg/kg)	1354±115	34	0.002

[a]Data are presented as the Mean ± SD; [b]compared to vehicle control.

Conclusions

Over the past years, we developed a focused library of furanopyrimidines which was rapidly synthesized using a variety of primary and secondary amines as nucleophiles in parallel reactors and *in situ* screened for EGFR kinase inhibitory activity to identify an initial hit (**1**). Very

interestingly, the initial hit (**1**) possesses an (*S*)-2-phenylglycinol functional group on the furanopyrimidine core as the key fragment for its bioactivity. Through hit-to-lead optimization, introduction of an acrylamide into the *meta*-position of the phenyl group in the 5-position of the furanopyrimidine core led to lead compound **2**, which showed enhanced potency in both enzymatic and cellular assays. However, lead **2** exhibited a poor pharmacokinetic profile and moderate inhibition of H1975 cell line. To improve these properties in this work, we have designed and synthesized a series of fused pyrimidine analogues using a scaffold hopping strategy and a structure-based drug design through lead-to-candidate optimization. In particular, compound **78**, which bears a *N*,*N*-dimethylamino group on the terminal double bond of acrylamide, showed a 2-fold improvement in H1975 activity compared to lead **2** while maintaining its inhibitory activity against HCC827 cells. Moreover, **78** showed 4-fold oral AUC better that afatinib along with F = 41.5% and exhibited excellent antitumor efficacy in both HCC827 and H1975 xenograft mouse models with minimal toxicity. Although, compound **78** belongs to 2nd-generation EGFR-TKIs similar to afatinib and dacomitinib, most interesting we identified furanopyrimidine **78** exhibited comparable potency to poziotinib, but 10-fold potency better than 3rd generation inhibitor, osimertinib, against three EGFR and one HER2 exon 20 insertion mutations, since there are currently no EGFR-directed therapies approved specifically for the treatment of both mutations. The outcome represent compound **78** is a potential new efficacious drug candidate in many cancers with EGFR or HER2 exon 20 mutations. X-ray co-

crystal study of $EGFR^{WT}$ kinase and compound **78** revealed the potential of future design for mutant-selective inhibitors. Finally, clinical candidate **78** was conducted all preclinical experiments and is currently undergoing phase 1 clinical trial (NCT03246854) in Taiwan.

Experimental section

General methods for Chemistry. All commercial chemicals and solvents are reagent-grade and were used without further purification unless otherwise stated. All reactions were carried out under dry nitrogen atmosphere and were monitored for completion by thin-layer chromatography (TLC) using Merck 60 F_{254} silica gel glass backed plates (5 ×10 cm); zones were detected visually under UV irradiation (254 nm) or by spraying with phosphomolybdic acid reagent (Aldrich) followed by heating at 80 °C. Flash column chromatography was carried out using silica gel (Merck Kieselgel 60, no. 9385, 230-400 mesh ASTM). ^{1}H and ^{13}C NMR spectra were obtained with a Varian Mercury-300, Varian Mercury-400 or Bruker DMX-600 spectrometers and the chemical shifts were recorded in parts per million (ppm, δ) and reported relative to TMS or the solvent peak. Low-resolution mass spectra (LRMS) were obtained with an Agilent MSD-1100 ESI-MS/MS system. High-resolution mass spectra (HRMS) were measured with a VARIAN 901-MS mass spectrometer. Purity of the final compounds were determined with a Hitachi 2000 series HPLC system using C-18 column (Agilent ZORBAX Eclipse XDB-C18 5 μm. 4.6 mm × 150 mm) operating at 25 °C. For method A, elution was

carried out using acetonitrile as mobile phase A, and water containing 0.1% formic acid + 10 mmol NH_4OAc as mobile phase B. Elution conditions: at 0 min, phase A 10% + phase B 90%; at 45 min, phase A 90% + phase B 10%; at 50 min, phase A 10% + phase B 90%; at 60 min, phase A 10% + phase B 90%. For method B, elution was carried out using acetonitrile as mobile phase A, and water containing 0.1% formic acid + 2 mmol NH_4OAc as mobile phase B. Elution conditions: at 0 min, phase A 10% + phase B 90%; at 25 min, phase A 90% + phase B 10%; at 30 min, phase A 90% + phase B 10%; at 30.5 min, phase A 10% + phase B 90%; at 37 min, phase A 10% + phase B 90%. The flow-rate of the mobile phase was 0.5 mL/min and the injection volume of the sample was 10 or 20 μL. Peaks were detected at 254 nm. The purity of all tested compounds was determined and confirmed to be greater than 95% by HPLC analysis except for compound **45** (93.5%), **71** (92.3%), **72** (90.8%), **74** (93.9%), **76** (93.6%), **82** (94.3%), and **83** (92.4%). IUPAC nomenclature of compounds were obtained with the software ACD/Name Pro. A JASCO P-1020 polarimeter with a sodium lamp was used for the determination of specific rotations at 25 °C. Melting points were obtained with an Electrothermal 9100 melting point apparatus.

***N*-[3-(4-{[(1*S*)-2-Hydroxy-1-phenylethyl]amino}furo[2,3-*d*]pyrimidin-5-yl)phenyl]prop-2-enamide (42).** A solution of **36** (48 mg, 0.14 mmol), acrylic acid (12 mg, 0.17 mmol) and EDCI·HCl (31 mg, 0.17 mmol) in CH_2Cl_2 (2 mL) was stirred at 0 °C for 1 h. The solution was quenched by water and extracted with dichloromethane. The organic layers were dried over

$MgSO_{4(s)}$ and concentrated to give a residue. The residue was purified by preparative layer chromatography (ethyl acetate/hexanes = 2:1) to give the product **42** (21 mg, 38%). ^{1}H NMR (300 MHz, $CDCl_3$): δ 8.24 (s, 1H), 8.04 (s, 1H), 7.65 (d, *J* = 8.1 Hz, 1H), 7.50–7.30 (m, 7H), 7.01 (s, 1H), 6.46–6.39 (m, 2H), 5.80 (dd, *J* = 9.6, 1.8 Hz, 1H), 5.38 (br s, 1H), 4.04–3.98 (m, 2H); ^{13}C NMR (100 MHz, $CDCl_3$+CD_3OD) δ 165.8, 164.8, 157.4, 153.2, 139.1, 139.0, 137.7, 131.2, 130.5, 129.8, 128.2, 127.6, 127.2, 126.2, 124.0, 120.7, 120.0, 119.7, 100.2, 65.4, 56.7; LC-MS (ESI) *m/z* 401.0 $[M + H]^+$; HRMS (ESI) calculated for $C_{23}H_{20}N_4O_3Na$: 423.1433 $[M + Na]^+$, found 423.1442; HPLC purity (method B): 97.7%, t_R = 19.31 min.

(*N*-[3-(4-{[(1*S*)-2-Hydroxy-1-phenylethyl]amino}-6-methylfuro[2,3-*d*]pyrimidin-5-yl)phenyl]prop-2-enamide (43). Compound **43** was prepared from acrylic acid and **37**, similarly to **42**. After work-up, the residue was purified by preparative layer chromatography (methanol/CH_2Cl_2 = 1:19) to give the product **43** (3.3 mg, 57%). ^{1}H NMR (300 MHz, DMSO-d_6): δ 10.34 (br s, 1H, NH), 8.21 (s, 1H), 7.98 (s, 1H), 7.69 (d, *J* = 8.1 Hz, 1H), 7.53 (dd, *J* = 8.1, 7.5 Hz, 1H), 7.26–7.17 (m, 6H), 6.47 (dd, *J* = 17.1, 9.9 Hz, 1H), 6.30 (dd, *J* = 17.1, 1.8 Hz, 1H), 5.92 (d, *J* = 7.5 Hz, 1H, NH), 5.80 (dd, *J* = 9.9, 1.8 Hz, 1H), 5.25–5.21 (m, 1H), 4.87 (t, *J* = 4.8 Hz, 1H, OH), 3.66–3.61 (m, 1H), 3.54–3.47 (m, 1H), 2.43 (s, 3H); ^{13}C NMR (100 MHz, $CDCl_3$+CD_3OD) δ 164.7, 164.6, 156.6, 152.5 148.2, 139.2, 138.9, 132.1, 130.7, 129.8, 128.5, 127.9, 127.4, 126.2, 125.2, 120.8, 119.8, 114.7, 101.8, 66.3, 56.9, 11.9; LC-MS (ESI) *m/z* 415.1

[M + H]$^+$; HRMS (ESI) calculated for $C_{24}H_{23}N_4O_3$: 415.1770 [M + H]$^+$, found 415.1772; HPLC purity (method B): 98.7%, t_R = 19.91 min.

***N*-[3-(4-{[(1*S*)-2-Hydroxy-1-phenylethyl]amino}thieno[2,3-*d*]pyrimidin-5-yl)phenyl]prop-2-enamide (44).** To a solution of **38** (16.3 mg, 0.045 mmol) and pyridine (5.5 μL, 0.067 mmol) in diethyl ether (5 mL) was added acryloyl chloride (5.5 μL, 0.067 mmol) at 0 °C in one portion. The reaction mixture was stirred at room temperature overnight. The solution was quenched by water and extracted with ethyl acetate. The combined organic layers were dried over $MgSO_{4(s)}$, and concentrated to give a residue. The residue was purified by preparative layer chromatography (methanol/CH_2Cl_2 = 1:15) to give the product **44** (4.6 mg, 25%) as a white solid. ^{1}H NMR (400 MHz, $CDCl_3$): δ 8.39 (s, 1H), 7.79 (d, *J* = 8.4 Hz, 1H), 7.71 (s, 1H), 7.44 (t, *J* = 8.0 Hz, 1H), 7.32 (s, 1H), 7.26–7.21 (m, 4H), 7.19 (s, 1H), 7.02 (d, *J* = 7.6 Hz, 2H), 6.45 (dd, *J* = 17.2, 1.6 Hz, 1H), 6.32 (dd, *J* = 17.2, 10.0 Hz, 1H), 5.94 (d, *J* = 6.8 Hz, 1H), 5.78 (dd, *J* = 10.0, 1.6 Hz, 1H), 5.32 (br s, 1H), 3.82–3.80 (m, 1H), 3.64–3.59 (m, 1H); ^{13}C NMR (75 MHz, $CDCl_3$+CD_3OD) δ 166.2, 164.6, 157.1, 157.0, 153.3, 138.9, 138.7, 136.3, 134.4, 130.7, 129.8, 128.5, 128.0, 127.5, 126.2, 125.0, 120.7, 114.3, 66.3, 56.7; LC-MS (ESI) *m/z* 417.0 [M + H]$^+$; HRMS (ESI) calculated for $C_{23}H_{20}N_4O_2SNa$: 439.1205 [M + Na]$^+$, found 439.1219; HPLC purity (method B): 98.6%, t_R = 19.17 min.

***N*-[3-(6-Chloro-4-{[(1*S*)-2-hydroxy-1-phenylethyl]amino}thieno[2,3-*d*]pyrimidin-5-yl)phenyl]prop-2-enamide (45).** Compound **45** was prepared from acrylic acid and **39**,

similarly to **42**. After work-up, the residue was purified by preparative layer chromatography (methanol/CH_2Cl_2 = 1:30) to give the product **45** (66 mg, 62%). ^{1}H NMR (400 MHz, $CDCl_3$): δ 8.41–8.40 (m, 1H), 7.73–7.44 (m, 3H), 7.26–7.22 (m, 4H), 6.97–6.93 (m, 2H), 6.51–6.39 (m, 1H), 6.31–6.09 (m, 1H), 5.86–5.79 (m, 1H), 5.70–5.53 (m, 1H), 5.35–5.17 (m, 1H), 3.84–3.60 (m, 2H); ^{13}C NMR (75 MHz, $CDCl_3$) δ 164.7, 163.6, 163.5, 163.4, 155.9, 153.7, 153.5, 139.1, 139.0, 138.6, 133.5, 133.3, 130.7, 130.4, 130.3, 130.1, 128.8, 128.8, 128.6, 128.3, 127.9, 127.6, 126.5, 126.2, 125.7, 125.6, 125.3, 122.4, 122.1, 120.6, 114.6, 67.4, 66.5, 57.7, 56.5; LC-MS (ESI) *m/z* 451.0 $[M + H]^+$; HRMS (ESI) calculated for $C_{23}H_{19}ClN_4O_2SNa$: 473.0815 $[M + Na]^+$, found 473.0809; HPLC purity (method A): 93.5%, t_R = 31.37 min.

***N*-[3-(4-{[(1*S*)-2-Hydroxy-1-phenylethyl]amino}-6-methylthieno[2,3-*d*]pyrimidin-5-yl)phenyl]prop-2-enamide (46).** Compound **46** was prepared from acrylic acid and **40**, similarly to **42**. After work-up, the residue was purified by preparative layer chromatography (methanol/CH_2Cl_2 = 1:15) to give the product **46** (97.9 mg, 86%). ^{1}H NMR (400 MHz, $CDCl_3$): δ 8.39–8.38 (m, 1H), 7.70–7.49 (m, 2H), 7.38–7.34 (m, 1H), 7.24–7.09 (m, 4H), 6.95–6.90 (m, 2H), 6.51–6.38 (m, 1H), 6.31–6.08 (m, 1H), 5.85–5.78 (m, 1H), 5.55–5.39 (m, 1H), 5.30–5.13 (m, 1H), 3.84–3.61 (m, 2H), 2.33 (s, 3H); ^{13}C NMR (75 MHz, $CDCl_3$) δ 164.6, 163.9, 163.8, 163.7, 156.2, 152.6, 152.3, 139.2, 138.8, 138.6, 135.5, 135.4, 133.5, 133.2, 130.9, 130.6, 129.9, 129.5, 129.4, 128.8, 128.6, 128.4, 128.0, 127.9, 127.8, 127.6, 126.2, 125.6, 122.3, 121.2, 120.7, 119.9, 115.6, 67.8, 66.9, 58.0, 56.9, 13.8; LC-MS (ESI) *m/z* 431.1 $[M + H]^+$; HRMS (ESI)

calculated for C24H22N4O2SNa: 453.1361 $[M + Na]^+$, found 453.1364; HPLC purity (method B): 97.3%, t_R = 20.13 min.

***N*-[3-(4-{[(1*S*)-2-{[*tert*-Butyl(dimethyl)silyl]oxy}-1-phenylethyl]amino}[1,2]oxazolo[5,4-*d*]pyrimidin-3-yl)phenyl]prop-2-enamide (47).** Compound **47** was prepared from acrylic acid and **41**, similarly to **42**. After work-up, the residue was purified by preparative layer chromatography (methanol/CH_2Cl_2 = 1:15) to give the product **47** (18.1 mg, 78%) as a white solid. ^{1}H NMR (300 MHz, $CDCl_3$): δ 8.46 (s, 1H), 8.05 (s, 1H), 7.99 (d, *J* = 8.1 Hz, 1H), 7.58 (dd, *J* = 8.1, 8.1 Hz, 1H), 7.49–7.46 (m, 1H), 7.35–7.24 (m, 5H), 6.4 (d, *J* = 7.2 Hz, 1H, NH), 6.48 (dd, *J* = 16.8, 1.8 Hz, 1H), 6.35 (dd, *J* = 16.8, 9.9 Hz, 1H), 5.81 (dd, *J* = 8.8, 1.8 Hz, 1H), 5.46–5.43 (m, 1H), 3.96 (dd, *J* = 10.5, 4.5 Hz, 1H), 3.83 (dd, *J* = 10.5, 4.8 Hz, 1H), 0.667 (s, 9H), −0.232 (s, 6H); LC-MS (ESI) *m/z* 516 $[M + H]^+$.

***N*-[3-(4-{[(1*S*)-2-Hydroxy-1-phenylethyl]amino}[1,2]oxazolo[5,4-*d*]pyrimidin-3-yl)phenyl]prop-2-enamide (48).** To a solution of **47** (18.1 mg, 0.0350 mmol) in THF (5.0 mL) was added 1.0 M of tetrabutylammonium fluoride solution in THF (0.350 mL, 0.350 mmol). The reaction mixture was stirred at room temperature for 1 h. The solution was quenched with water and extracted with ethyl acetate. The organic layers were washed with brine, dried over $MgSO_{4(s)}$, filtered and concentrated to afford a residue. The residue was purified by preparative layer chromatography (methanol/CH_2Cl_2 = 1:15) to give the product **48** (13.1 mg, 93%) as a white solid. ^{1}H NMR (400 MHz, $CDCl_3$): δ 8.46 (s, 1H), 8.22 (s, 1H), 7.74–7.71 (m, 1H), 7.58–

7.57 (m, 2H), 7.31–7.22 (m, 5H), 6.47 (dd, *J* = 17.2, 1.2 Hz, 1H), 6.35 (dd, *J* = 17.2, 10.0 Hz, 1H), 5.82 (dd, *J* = 10.0, 1.2 Hz, 1H), 5.61–5.58 (m, 1H), 3.99 (dd, *J* = 11.8, 3.6 Hz, 1H), 3.86 (dd, *J* = 11.8, 5.1 Hz, 1H); ^{13}C NMR (75 MHz, $CD_3OD/CDCl_3$) δ 176.6, 166.3, 159.6, 159.3, 158.7, 141.2, 140.7, 132.1, 131.6, 130.2, 129.5, 128.6, 128.5, 127.9, 125.0, 123.4, 120.8, 96.1, 65.8, 58.4; LC-MS (ESI) *m/z* 402.1 $[M + H]^+$; HRMS (ESI) calculated for $C_{22}H_{19}N_5O_3Na$: 424.1386 $[M + Na]^+$, found 424.1383; HPLC purity (method A): 99.7%, t_R = 25.66 min.

(2*S*)-2-[(5-Bromo-6-phenylfuro[2,3-*d*]pyrimidin-4-yl)amino]-2-phenylethanol (56). A solution of 5-bromo-4-chloro-6-phenylfuro[2,3-*d*]pyrimidine (**52**[36], 20 g, 65 mmol), triethyamine (46 mL, 0.33 mol) and (*S*)-(+)-phenylglycinol (10.6 g, 77.2 mmol) in ethanol (185 mL) was refluxed overnight. The reaction solution was cooled and concentrated, water was added, and then it was extracted with ethyl acetate. The combined organic layers were dried over $MgSO_{4(s)}$, filtered, and concentrated to give the residue. The residue was purified by flash column chromatography (ethyl acetate/hexanes = 1:9) to give the product **56** (10 g, 37%). $[\alpha]_D^{25}$ = −223.96° (*c* = 0.25, CH_2Cl_2); ^{1}H NMR (400 MHz, $CDCl_3$): δ 8.33 (s, 1H), 8.08–8.06 (m, 2H), 7.51–7.30 (m, 8H), 6.89 (d, 1H), 5.50–5.45 (m, 1H), 4.08–4.05 (m, 2H), 3.39 (t, *J* = 6.0 Hz, 1H); ^{13}C NMR (100 MHz, $CDCl_3$) δ 164.0, 156.8, 154.2, 147.0, 139.1, 129.4, 129.0, 128.7, 128.2, 127.9, 126.5, 126.5, 102.7, 88.8, 67.1, 57.2; LC-MS (ESI) *m/z* 410, 412 $[M + H]^+$; HRMS (EI) calculated for $C_{20}H_{16}BrN_3O_2$: 409.0426 $[M]^+$, found 409.0412.

(2*S*)-2-{[5-(3-Nitrophenyl)-6-phenylfuro[2,3-*d*]pyrimidin-4-yl]amino}-2-phenylethanol (61). To a solution of **56** (4.60 g, 11.2 mmol) in 1,4-dioxane (10 mL) was added 3-nitrophenylboronic acid (1.87 g, 11.2 mmol), $Pd(dppf)_2Cl_2$ (0.90 g, 1.1 mmol) and 2.0 M $Na_2CO_{3(aq)}$ (10 mL, 20 mmol). The reaction was degassed, refilled with $argon_{(g)}$ and stirred at reflux overnight. The mixture was quenched by water and extracted with ethyl acetate. The combined organic layers were dried over $MgSO_{4(s)}$, filtered and concentrated to give a residue. The residue was purified by flash column chromatography (ethyl acetate/hexane = 1:3) to give the product **61** (2.14 g, 43%). $[\alpha]_D^{25} = -226.92°$ (c = 0.25, CH_2Cl_2); ^{1}H NMR (400 MHz, $CDCl_3$): δ 8.41 (s, 1H), 8.40 (s, 1H), 8.32–8.29 (m, 1H), 7.82 (d, J = 7.6 Hz, 1H), 7.65 (t, J = 8.0 Hz, 1H), 7.51–7.48 (m, 2H), 7.33–7.26 (m, 6H), 7.10–7.08 (m, 2H), 5.25–5.20 (m, 2H), 3.86–3.84 (m, 2H), 3.27 (t, J = 5.6 Hz, 1H); ^{13}C NMR (100 MHz, $CDCl_3$) δ 165.1, 156.8, 154.0, 148.8, 138.9, 136.1, 134.1, 130.8, 129.3, 128.9, 128.8, 128.5, 128.1, 126.7, 126.2, 124.5, 123.7, 112.4, 102.9, 67.2, 57.7; LC-MS (ESI) *m/z* 453.1 $[M + H]^+$; HRMS (EI) calculated for $C_{26}H_{20}N_4O_4$: 452.1485 $[M]^+$, found 452.1491.

(2*S*)-2-{[5-(3-Aminophenyl)-6-phenylfuro[2,3-*d*]pyrimidin-4-yl]amino}-2-phenylethanol (66). A solution of **61** (2.14 g, 4.73 mmol) and iron powder (2.10 g, 37.6 mmol) in ethanol (16 mL), acetic acid (16 mL) and water (8 mL) was stirred at 90 °C for 2 h. The solution was cooled and concentrated to give a residue. The residue was treated with water and extracted with CH_2Cl_2. The combined organic layers were dried over $MgSO_{4(s)}$, filtered, and concentrated to

obtain a residue. The residue was purified by flash column chromatography (methanol:CH_2Cl_2 = 1:30, containing 0.10% $NH_{3(aq)}$) to give the product **66** (1.57 g, 79%). $[\alpha]_D^{25}$ = −185.04° (*c* = 0.25, CH_2Cl_2); ^{1}H NMR (400 MHz, $CDCl_3$) δ 8.36 (s, 1H), 7.63 (dd, *J* = 7.6, 1.6 Hz, 2H), 7.34–7.27 (m, 8H), 7.10–7.07 (m, 2H), 6.76–6.63 (m, 2H), 5.62 (d, *J* = 5.2 Hz, 1H), 5.26 (td, *J* = 6.4, 3.6 Hz, 1H), 4.00–3.69 (m, 4H); ^{13}C NMR (100 MHz, $CDCl_3$) δ 164.5, 156.9, 153.1, 147.5, 147.0, 138.8, 132.9, 130.8, 129.3, 128.9, 128.6, 128.5, 127.9, 126.3, 110.5, 115.5, 115.1, 103.7, 67.9, 58.1; LC-MS (ESI) *m/z* 423.0 $[M + H]^+$; HRMS (EI) calculated for $C_{26}H_{22}N_4O_2$: 422.1743 $[M]^+$, found 422.1728.

***N*-[3-(6-Phenyl-4-{[(1*R*)-1-phenylethyl]amino}furo[2,3-*d*]pyrimidin-5-yl)phenyl]prop-2-enamide (70).** To a solution of **65** (51 mg, 0.12 mmol) and pyridine (11 mg, 0.12 mmol) in diethylether (2.0 mL) was added acryloyl chloride (16 mg, 0.20 mmol) at 0 °C. The solution was stirred at room temperature for 2 h, then it was quenched by water and extracted with ethyl acetate. The combined organic layers were dried over $MgSO_{4(s)}$, filtered and concentrated to give a residue. The residue was purified by preparative layer chromatography (ethyl acetate/hexanes = 1:2) to give the product **70** (89 mg, 11%). ^{1}H NMR (300 MHz, $CDCl_3$) δ 8.38 (s, 1H), 7.94 (d, 1H), 7.55–7.47 (m, 4H), 7.30–7.18 (m, 6H), 7.13–7.11 (m, 2H), 6.96 (d, *J* = 6.9 Hz, 1H), 6.46 (dd, *J* = 16.8, 1.2 Hz, 1H), 6.23 (dd, *J* = 16.8, 10.2 Hz, 1H), 5.80 (dd, *J* = 10.2, 1.2 Hz, 1H), 5.31 (quint, *J* = 6.9 Hz, 1H), 5.05 (d, *J* = 7.5 Hz, 1H), 1.39 (d, *J* = 6.9 Hz, 3H); ^{13}C NMR (100 MHz, $CDCl_3$) δ 164.5, 163.9, 156.6, 153.9, 146.6, 143.3, 139.6, 132.9,

130.9, 130.4, 129.0, 128.6, 128.5, 128.2, 127.2, 126.2, 125.6, 125.2, 120.5, 120.2, 114.4, 103.1, 50.3, 22.8; LC-MS (ESI) *m/z* 461.2 [M + H]$^+$; HRMS (ESI) calculated for $C_{29}H_{24}N_4O_2Na$: 483.1797 [M + Na]$^+$, found 483.1791; HPLC purity (method B): 97.9%, t_R = 28.69 min.

***N*-[3-(4-{[(1*S*)-2-Hydroxy-1-phenylethyl]amino}-6-phenylfuro[2,3-*d*]pyrimidin-5-yl)phenyl]but-2-ynamide (71).** A solution of **66** (211 mg, 0.499 mmol), 2-butynoic acid (51.0 mg, 0.607 mmol), and EDCI·HCl (115 mg, 0.600 mmol) in CH_2Cl_2 (5 mL) was stirred at room temperature overnight. The solution was concentrated and purified by preparative layer chromatography (ethyl acetate/hexanes = 3:2) to obtain product **71** (83.0 mg, 34% yield). ^{1}H NMR (300 MHz, $CDCl_3$): δ 8.37 (s, 1H), 7.67–7.53 (m, 4H), 7.43 (br t, 1H), 7.29–7.22 (m, 7H), 7.08–7.05 (m, 2H), 5.48 (br s, 1H), 5.30 (br s, 1H), 3.88–3.75 (m, 2H), 2.02 (s, 3H); ^{13}C NMR (100 MHz, $CDCl_3$) δ 164.8, 157.4, 153.7, 151.7, 147.3, 139.3, 139.0, 133.1, 130.9, 130.8, 129.2, 129.0, 128.9, 128.7, 128.0, 126.6, 126.4, 126.2, 120.8, 114.4, 103.6, 85.5, 75.4, 67.4, 57.7, 3.95;LC-MS (ESI) *m/z* 489.1 [M + H]$^+$; HRMS (ESI) calculated for $C_{30}H_{24}N_4O_3Na$: 511.1746 [M + Na]$^+$, found 511.1747; HPLC purity (method B): 92.3%, t_R = 24.19 min.

***N*-[3-(4-{[(1*S*)-2-Hydroxy-1-phenylethyl]amino}-6-phenylfuro[2,3-*d*]pyrimidin-5-yl)phenyl]ethenesulfonamide (72).** To a solution of **66** (200 mg, 0.473 mmol) and triethylamine (0.50 mL) in CH_2Cl_2 (5.0 mL) was added 2-chloroethanesulfonyl chloride (0.30 mL, 2.87 mmol) at room temperature. The solution was stirred at room temperature for 4 h and concentrated. The crude was treated with by water and CH_2Cl_2. The organic layer was dried

over $MgSO_{4(s)}$, filtered, and concentrated to obtain a residue. The residue was purified by flash column chromatography (2.5–5% methanol in CH_2Cl_2 containing 0.10% $NH_{3(aq)}$) to give the product **72** (4.7 mg, 2%). ^{1}H NMR (400 MHz, CD_3OD-d_4) δ 8.24 (s, 1H), 7.59–7.51 (m, 3H), 7.42–7.21 (m, 9H), 7.16 (d, *J* = 8.4 Hz, 1H), 6.62 (dd, 1H), 6.10 (d, *J* = 16.8 Hz, 1H), 5.85 (d, *J* = 9.6 Hz, 1H), 5.27 (dd, *J* = 5.2, 4.8 Hz, 1H), 3.76 (dd, *J* = 11.2 4.8 Hz, 1H), 3.64 (dd, *J* = 11.2, 5.2 Hz, 1H); ^{13}C NMR (75 MHz, $CDCl_3$) δ 164.5, 157.2, 153.7, 147.1, 139.0, 138.4, 135.3, 133.3, 130.9, 128.9, 128.8, 128.7, 128.5, 128.3, 127.8, 126.3, 126.2, 125.8, 121.1, 120.4, 114.0, 103.3, 67.0, 57.2; LC-MS (ESI) *m/z* 513.1 $[M + H]^+$; HRMS (ESI) calculated for $C_{28}H_{24}N_4O_4SNa$: 535.1416 $[M + Na]^+$, found 535.1420; HPLC purity (method B): 90.8%, t_R = 24.11 min.

(2*E*)-*N*-[3-(4-{[(1*S*)-2-Hydroxy-1-phenylethyl]amino}-6-phenylfuro[2,3-*d*]pyrimidin-5-yl)phenyl]but-2-enamide (73). Compound **73** was prepared from (*E*)-but-2-enoic acid and **66**, similarly to **71**. After work-up, the residue was purified by flash column chromatography (5% methanol in CH_2Cl_2 containing 0.10% $NH_{3(aq)}$ to give the product **73** (77.9 mg, 67%). ^{1}H NMR (400 MHz, DMSO-d_6) δ 10.17 (s, 1H, NH), 8.28 (s, 1H), 7.97 (s, 1H), 7.80 (d, *J* = 8.4 Hz, 1H), 7.62–7.14 (m, 11H), 6.84–6.77 (m, 2H), 6.12 (d, *J* = 15.2 Hz, 1H), 5.75 (d, 1H, NH), 5.25–5.20 (m, 1H), 4.82 (t, *J* = 4.8 Hz, 1H, OH), 3.63–3.56 (m, 1H), 3.47–3.38 (m, 1H), 1.87 (d, *J* = 6.8 Hz, 3H); ^{13}C NMR (100 MHz, $CDCl_3$) δ 164.8, 164.5, 157.4, 153.9, 147.0, 142.9, 139.3, 139.0, 132.8, 133.1, 130.5, 129.2, 128.7, 128.6, 128.5, 127.6, 126.5, 126.3, 126.0, 124.7, 121.3, 120.8,

114.4, 103.5, 67.2, 57.3, 17.9; LC-MS (ESI) *m/z* 491.2 $[M + H]^+$; HRMS (ESI) calculated for $C_{30}H_{26}N_4O_3Na$: 513.1903 $[M + Na]^+$, found 513.1904; HPLC purity (method B): 96.2%, t_R = 24.79 min.

(2*E*)-*N*-[3-(4-{[(1*S*)-2-Hydroxy-1-phenylethyl]amino}-6-phenylfuro[2,3-*d*]pyrimidin-5-yl)phenyl]-5-methylhex-2-enamide (74). Compound **74** was prepared from (2*E*)-5-methyl-2-hexenoic acid and **66**, similarly to **71**. After work-up, the residue was purified by flash column chromatography (methanol/CH_2Cl_2 = 1:40) to give the product **74** (60 mg, 45%). ^{1}H NMR (400 MHz, $CDCl_3$) δ 8.38 (s, 1H), 7.82–7.60 (m, 2H), 7.58–7.50 (m, 2H), 7.48–7.39 (m, 1H), 7.32–7.17 (m, 7H), 7.10–6.93 (m, 3H), 5.83 (d, *J* = 15.6 Hz, 1H), 5.60 (br s, 1H), 5.38 (br s, 1H), 3.94–3.82 (m, 1H), 3.80–3.70 (m, 1H), 2.18–2.08 (m, 2H), 1.83–1.71 (m, 1H), 0.98–0.88 (m, 6H); ^{13}C NMR (100 MHz, $CDCl_3$) δ 164.7, 164.6, 157.3, 153.6, 147.0, 146.4, 139.2, 132.8, 130.5, 129.1, 128.7, 128.6, 128.5, 127.6, 126.4, 126.2, 125.7, 124.4, 121.2, 120.8, 114.5, 103.4, 67.0, 57.3, 41.4, 27.7, 22.2; LC-MS (ESI) *m/z* 533.2 $[M + H]^+$; HRMS (ESI) calculated for $C_{33}H_{32}N_4O_3Na$: 555.2372 $[M + Na]^+$, found 555.2368; HPLC purity (method A): 93.9%, t_R = 42.71 min.

(2*E*)-*N*-[3-(4-{[(1*S*)-2-Hydroxy-1-phenylethyl]amino}-6-phenylfuro[2,3-*d*]pyrimidin-5-yl)phenyl]-3-phenylprop-2-enamide (75). Compound **75** was prepared from *trans*-cinnamic acid and **66**, similarly to **71**. After work-up, the residue was purified by flash column chromatography (5% methanol in CH_2Cl_2 containing 0.10% $NH_{3(aq)}$) to give the product **75**

(62.5 mg, 48%). ^{1}H NMR (400 MHz, DMSO-d_6) δ 10.45 (s, 1H, NH), 8.29 (s, 1H), 8.01 (s, 1H), 7.89 (d, J = 8.0 Hz, 1H), 7.64–7.16 (m, 18H), 6.84 (d, J = 15.6 Hz, 1H), 5.77 (d, 1H, NH), 5.24–5.19 (m, 1H), 4.84 (t, J = 4.8 Hz, 1H, OH), 3.63–3.58 (m, 1H), 3.47–3.41 (m, 1H); ^{13}C NMR (75 MHz, $CDCl_3$) δ 164.9, 164.6, 157.3, 153.6, 147.0, 142.9, 139.4, 139.2, 134.3, 132.8, 130.5, 130.1, 129.7, 129.0, 128.8, 128.7, 128.5, 127.9, 127.6, 126.4, 126.2, 125.8, 121.1, 120.7, 120.3, 114.4, 103.4, 66.9, 57.2; LC-MS (ESI) *m/z* 553.2 $[M + H]^+$; HRMS (ESI) calculated for $C_{35}H_{28}N_4O_3Na$: 575.2059 $[M + Na]^+$, found 575.2065; HPLC purity (method A): 99.1%, t_R = 41.19 min.

(2*E*)-4-{[3-(4-{[(1*S*)-2-Hydroxy-1-phenylethyl]amino}-6-phenylfuro[2,3-*d*]pyrimidin-5-yl)phenyl]amino}-4-oxobut-2-enoic acid (76). Compound **76** was prepared from *trans*-2-butenedioic acid and **66**, similarly to **71**. After work-up, the residue was purified by flash column chromatography (5% methanol in CH_2Cl_2 containing 0.10% $NH_{3(aq)}$) to give the product **76** (39.5 mg, 33%). ^{1}H NMR (300 MHz, CD_3OD-d_4) δ 8.25 (s, 1H), 7.98 (s, 1H), 7.87 (d, J = 8.1 Hz, 1H), 7.61–7.56 (m, 3H), 7.32–7.14 (m, 9H), 7.02 (d, J = 15.3 Hz, 1H), 6.87 (d, J = 15.3 Hz, 1H), 5.26 (dd, J = 5.1, 4.8 Hz, 1H), 3.75 (dd, J = 10.8, 4.8 Hz, 1H), 3.62 (dd, J = 10.8, 5.1 Hz, 1H); ^{13}C NMR (75 MHz, CD_3OD-d_4) δ 168.6, 165.8, 164.6, 158.6, 154.9, 148.5, 141.4, 141.3, 137.8, 134.2, 131.9, 130.6, 130.1, 129.9, 129.7, 128.6, 127.9, 127.6, 127.1, 122.2, 121.7, 116.4, 104.6, 66.93, 57.7; LC-MS (ESI) m/z 521.2 $[M + H]^+$; HRMS (ESI) calculated for

$C_{30}H_{24}N_4O_5Na$: 543.1644 [M + Na]$^+$, found 543.1626; HPLC purity (method A): 93.6%, t_R = 43.58 min.

Ethyl (2*E*)-4-{[3-(4-{[(1*S*)-2-hydroxy-1-phenylethyl]amino}-6-phenylfuro[2,3-*d*]pyrimidin-5-yl)phenyl]amino}-4-oxobut-2-enoate (77). Compound **77** was prepared from *trans*-2-butenedioic acid and **66**, similarly to **71**. After work-up, the residue was purified by flash column chromatography (5% methanol in CH_2Cl_2 containing 0.10% $NH_{3(aq)}$) to give the product **77** (52.6 mg, 40%). ^{1}H NMR (400 MHz, DMSO-d_6) δ 10.78 (s, 1H, NH), 8.28 (s, 1H), 8.02 (s, 1H), 7.83 (d, *J* = 8.4 Hz, 1H), 7.60 (t, *J* = 8.0 Hz, 1H), 7.53–7.51 (m, 2H), 7.41–7.15 (m, 10H), 6.71 (d, *J* = 15.2 Hz, 1H), 5.75 (d, *J* = 7.6 Hz, 1H), 5.22–5.17 (m, 1H), 4.83 (t, *J* = 4.8 Hz, 1H, OH), 4.21 (q, *J* = 7.2 Hz, 2H), 3.62–3.57 (m, 1H), 3.45–3.40 (m, 1H), 1.26 (t, *J* = 7.2 Hz, 3H); ^{13}C NMR (100 MHz, $CDCl_3$) δ 165.6, 164.5, 162.2, 157.2, 153.5, 147.1, 139.1, 139.0, 136.5, 132.8, 131.5, 130.6, 128.9, 128.7, 128.6, 128.5, 127.7, 126.3, 126.2, 120.9, 120.7, 114.2, 103.3, 66.8, 61.4, 57.2, 14.0; LC-MS (ESI) *m/z* 549.3 [M + H]$^+$; HRMS (ESI) calculated for $C_{32}H_{28}N_4O_5Na$: 571.1957 [M + Na]$^+$, found 571.1967; HPLC purity (method A): 98.6%, t_R = 37.99 min.

(2*E*)-4-(Dimethylamino)-*N*-[3-(4-{[(1*S*)-2-hydroxy-1-phenylethyl]amino}-6-phenylfuro[2,3-*d*]pyrimidin-5-yl)phenyl]but-2-enamide (78). To a solution of **66** (20.00 g, 47.34 mmol) in CH_2Cl_2 (400 mL) was added 4-bromocrotonoic acid (8.59 g, 52.07 mmol) and EDCI·HCl (14.52 g, 75.74 mmol), and it was stirred at room temperature overnight. The

solution was concentrated and then was added by THF (400 mL) and dimethylamine (40 wt % in water, 30.30 mL, 236.7 mmol) and continued stirring for 8 h. The resulting solution was concentrated and partitioned with CH_2Cl_2 (500 mL x 4) and saturated $NaHCO_{3(aq)}$. The combined organic layers were dried over $MgSO_{4(s)}$, filtered and concentrated *in vacuo*. The residue was purified by flash column chromatography (methanol:acetone= 1:20) to give the product **78** (12.56 g, 50%) as a pale yellow solid. mp: 185–186 °C; $[\alpha]_D^{25}$ = −265.3° (*c* = 0.25, CH_2Cl_2); ^{1}H NMR (400 MHz, DMSO-d_6): δ 10.28 (s, 1H), 8.27 (s, 1H), 7.98 (br s, 1H), 7.81 (d, *J* = 8.0 Hz, 1H), 7.55 (t, *J* = 8.0 Hz, 1H), 7.53–7.50 (m, 2H), 7.40–7.13 (m, 9H), 6.74 (dt, *J* = 15.4, 5.8 Hz, 1H), 6.28 (d, *J* = 15.4 Hz, 1H), 5.49 (d, *J* = 8.0 Hz, 1H), 5.23–5.19 (m, 1H), 4.81 (br t, *J* = 4.8 Hz, 1H), 3.60–3.55 (m, 1H), 3.44–3.39 (m, 1H), 3.05 (d, *J* = 5.8 Hz, 1H), 2.16 (s, 6H); ^{13}C NMR (150 MHz, DMSO-d_6) δ 164.5, 163.7, 156.7, 154.1, 145.8, 142.0, 140.8, 140.6, 132.0, 130.6, 129.0, 129.0, 128.9, 128.2, 127.0, 126.6, 126.0, 125.8, 124.3, 119.8, 119.7, 115.2, 102.7, 64.5, 59.8, 55.5, 45.2; LC-MS (ESI) *m/z* 534.1 $[M + H]^+$; HRMS (ESI) calculated for $C_{32}H_{32}N_5O_3$: 534.2505 $[M + H]^+$, found 534.2474; HPLC purity (method B): 95.7%, t_R = 16.01 min.

(2*E*)-4-(Diethylamino)-*N*-[3-(4-{[(1*S*)-2-hydroxy-1-phenylethyl]amino}-6-phenylfuro[2,3-*d*]pyrimidin-5-yl)phenyl]but-2-enamide (79). Compound **79** was prepared from 4-bromocrotonoic acid, *N*,*N*-diethylamine and **66**, similarly to **78**. After work-up, the residue was purified by flash column chromatography (5% methanol in CH_2Cl_2 containing 0.10% $NH_{3(aq)}$)

to give the product **79** (43.7 mg, 32%). ^{1}H NMR (300 MHz, $CDCl_3$): δ 8.30 (s, 1H), 7.77–7.75 (m, 2H), 7.53–7.48 (m, 2H), 7.41 (dd, *J* = 8.4, 7.5 Hz, 1H), 7.27–7.17 (m, 7H), 7.11–7.00 (m, 2H), 6.97 (dt, *J* = 15.3, 5.7 Hz, 1H), 6.17 (d, *J* = 15.3 Hz, 1H), 5.68 (d, *J* = 6.6 Hz, 1H), 5.33 (br s, 1H), 3.89–3.84 (m, 1H), 3.72–3.63 (m, 1H), 3.24 (d, *J* = 5.7 Hz, 2H), 2.54 (q, *J* = 7.2 Hz, 4H), 1.02 (t, *J* = 7.2 Hz, 6H); ^{13}C NMR (75 MHz, $CDCl_3$) δ 164.6, 164.3, 157.2, 153.7, 146.9, 142.7, 139.4, 132.8, 130.5, 129.1, 128.6, 128.5, 127.5, 126.4, 126.3, 126.0, 125.7, 121.0, 120.8, 114.5, 103.3, 66.6, 57.0, 53.8, 47.0, 11.4; LC-MS (ESI) *m/z* 562.3 $[M + H]^+$; HRMS (ESI) calculated for $C_{34}H_{36}N_5O_3$: 562.2818 $[M + H]^+$, found 562.2841; HPLC purity (method A): 97.0%, t_R = 24.47 min.

(2*E*)-4-[Ethyl(2-hydroxyethyl)amino]-*N*-[3-(4-{[(1*S*)-2-hydroxy-1-phenylethyl]amino}-6-phenylfuro[2,3-*d*]pyrimidin-5-yl)phenyl]but-2-enamide (80). Compound **80** was prepared from 4-bromocrotonoic acid, 2-(ethylamino)ethanol and **66**, similarly to **78**. After work-up, the residue was purified by flash column chromatography (5% methanol in CH_2Cl_2 containing 0.10% NH_3(aq)) to give the product **80** (35.7 mg, 26%). ^{1}H NMR (300 MHz, $CDCl_3$): δ 8.33 (s, 1H), 7.79–7.72 (m, 2H), 7.55–7.52 (m, 2H), 7.42 (t, *J* = 7.8 Hz, 1H), 7.27–7.20 (m, 7H), 7.08–7.06 (m, 2H), 6.94 (dt, *J* = 15.3, 5.7 Hz, 1H), 6.15 (d, *J* = 15.3 Hz, 1H), 5.69 (d, *J* = 6.6 Hz, 1H), 5.34 (br s, 1H), 3.84 (dd, *J* = 11.4, 3.3 Hz, 1H), 3.69 (dd, *J* = 11.4, 6.0 Hz, 1H), 3.57 (t, *J* = 5.4 Hz, 2H), 3.31 (d, *J* = 5.7 Hz, 2H), 2.64–2.52 (m, 4H), 1.05 (t, *J* = 7.2 Hz, 3H); ^{13}C NMR (100 MHz, $CDCl_3$) δ 169.4, 164.8, 157.3, 157.28, 153.9, 146.9, 139.4, 139.0, 133.1, 130.5,

130.46, 129.3, 128.7, 128.6, 128.5, 127.6, 126.5, 126.3, 125.9, 121.1, 120.6, 114.5, 103.5, 72.6, 66.9, 57.4, 52.3, 41.6, 29.67, 11.5; LC-MS (ESI) *m/z* 578.3 $[M + H]^+$; HRMS (ESI) calculated for $C_{34}H_{36}N_5O_4$: 578.2767 $[M + H]^+$, found 578.2764; HPLC purity (method B): 96.8%, t_R = 16.65 min.

(2*E*)-*N*-[3-(4-{[(1*S*)-2-Hydroxy-1-phenylethyl]amino}-6-phenylfuro[2,3-*d*]pyrimidin-5-yl)phenyl]-4-(morpholin-4-yl)but-2-enamide (81). Compound **81** was prepared from 4-bromocrotonoic acid, morpholine and **66**, similarly to **78**. After work-up, the residue was purified by flash column chromatography (3.3% methanol in CH_2Cl_2) to give the product **81** (201 mg, 26%). ^{1}H NMR (300 MHz, CD_3OD-d_4): δ 8.24 (s, 1H), 7.94 (s, 1H), 7.83 (d, *J* = 8.4 Hz, 1H), 7.58–7.54 (m, 3H), 7.32–7.13 (m, 9H), 6.90 (dt, *J* = 15.3, 5.7 Hz, 1H), 6.31 (d, *J* = 15.3 Hz, 1H), 5.27 (t, *J* = 5.1 Hz, 1H), 3.69–3.58 (m, 6H), 3.21 (d, *J* = 5.7 Hz, 2H), 2.52–2.49 (m, 4H); ^{13}C NMR (100 MHz, $CDCl_3$) δ 164.5, 164.1, 157.2, 153.6, 147.0, 141.9, 139.3, 139.25, 132.8, 130.5, 129.0, 128.6, 128.5, 127.6, 126.3, 126.2, 126.0, 125.8, 121.0, 120.8, 114.4, 103.4, 66.7, 59.4, 57.0, 53.6; LC-MS (ESI) *m/z* 576.0 $[M + H]^+$; HRMS (ESI) calculated for $C_{34}H_{34}N_5O_4$: 576.2611 $[M + H]^+$, found 576.2608; HPLC purity (method A): 98.3%, t_R = 23.79 min.

***N*-{3-[4-{[(1*S*)-2-Hydroxy-1-phenylethyl]amino}-6-(2-methoxyphenyl)furo[2,3-*d*]pyrimidin-5-yl]phenyl}prop-2-enamide (82).** Compound **82** was prepared from acrylic acid and **68**, similarly to **71**. After work-up, the residue was purified by preparative layer

chromatography (5% methanol in CH_2Cl_2) to give the product **82** (6.7 mg, 66% yield). ^{1}H NMR (400 MHz, DMSO-d_6): δ 10.25 (s, 1H, NH), 8.27 (s, 1H), 7.84 (s, 1H), 7.69 (d, J = 8.0 Hz, 1H), 7.44–7.38 (m, 3H), 7.28–7.20 (m, 5H), 7.11–7.05 (m, 2H), 7.01–6.97 (m, 1H), 6.43 (dd, J = 16.8, 10.0 Hz, 1H), 6.26 (dd, J = 16.8, 2.0 Hz,, 1H), 5.96 (d, J = 7.2 Hz, 1H, NH), 5.76 (dd, J = 10.0, 2.0 Hz, 1H), 5.27–5.25 (m, 1H), 4.87 (t, J = 4.8 Hz, 1H), 3.65–3.47 (m, 2H), 3.51 (s, 3H); ^{13}C NMR (75 MHz, $CDCl_3$) δ 165.0, 163.4, 157.1, 156.5, 153.6, 145.1, 140.9, 139.7, 132.7, 131.8, 131.3, 131.2, 129.6, 128.2, 127.2, 126.9, 126.7, 124.0, 120.4, 119.4, 118.8, 117.7, 116.8, 111.9, 11.5, 64.4, 55.7, 55.1; LC-MS (ESI) *m/z* 507.2 $[M + H]^+$; HRMS (ESI) calculated for $C_{30}H_{27}N_4O_4$: 507.2032 $[M + H]^+$, found 507.2034; HPLC purity (method A): 94.3%, t_R = 32.05 min.

***N*-[3-(4-{[(1*R*)-2-Hydroxy-1-phenylethyl]amino}-6-phenylfuro[2,3-*d*]pyrimidin-5-yl)phenyl]prop-2-enamide (83).** Compound **83** was prepared from acrylic acid and **67**, similarly to **82**. After work-up, the residue was purified by CombiFlash automated flash chromatography (0–10% methanol in CH_2Cl_2) to give the product **83** (75 mg, 65%) as a white solid. ^{1}H NMR (400 MHz, $CDCl_3$): δ 8.35 (s, 1H), 7.73 (br m, 2H), 7.54–7.51 (m, 2H), 7.44 (dd, J = 8.0, 7.6 Hz, 1H), 7.28–7.20 (m, 7H), 7.07–7.04 (m, 2H), 6.48 (d, J = 16.8 Hz, 1H), 6.26 (br dd, 1H), 5.82 (d, J = 4.0 Hz, 1H), 5.56 (br s, 1H), 5.33 (br s, 1H), 3.89–3.86 (m, 1H), 3.76–3.72 (m, 1H); ^{13}C NMR (100 MHz, $CDCl_3$) δ 164.4, 164.3, 157.2, 153.4, 147.0, 139.3, 139.1, 132.6, 130.7, 130.5, 128.9, 128.6, 128.4, 128.3, 127.6, 126.3, 126.2, 125.8, 121.0, 120.8, 114.4,

103.3, 66.6, 57.1; LC-MS (ESI) *m/z* 477.2 [M + H]$^+$; HRMS (ESI) calculated for $C_{29}H_{24}N_4O_3Na$: 499.1746 [M + Na]$^+$, found 499.1745; HPLC purity (method B): 92.4%, t_R = 23.81 min.

(2*E*)-4-(Dimethylamino)-*N*-[3-(4-{[(1*R*)-2-hydroxy-1-phenylethyl]amino}-6-phenylfuro[2,3-*d*]pyrimidin-5-yl)phenyl]but-2-enamide (84). Compound **84** was prepared from 4-bromocrotonoic acid, *N*,*N*-dimethylamine and **67**, similarly to **78**. After work-up, the residue was purified by CombiFlash automated flash chromatography (0–10% methanol in CH_2Cl_2) to give the product **84** (135 mg, 60%) as a white solid. ^{1}H NMR (400 MHz, $CDCl_3$): δ 8.37 (s, 1H), 7.88–7.61 (br m, 2H), 7.56–7.54 (m, 2H), 7.44 (br t, 1H), 7.30–7.22 (m, 7H), 7.12–6.95 (m, 3H), 6.17 (d, *J* = 16.8 Hz, 1H), 5.64 (br s, 1H), 5.35 (br s, 1H), 3.89–3.86 (m, 1H), 3.75–3.71 (m, 1H), 3.09 (d, *J* = 5.2 Hz, 2H), 2.26 (s, 6H); ^{13}C NMR (75 MHz, $CDCl_3$) δ 164.8, 164.1, 157.3, 153.9, 147.0, 141.8, 139.4, 139.1, 133.0, 130.6, 129.2, 128.7, 128.6, 127.6, 126.5, 126.3, 126.1, 121.2, 120.9, 114.4, 103.4, 66.9, 60.0, 57.2, 45.2; LC-MS (ESI) *m/z* 534.3 [M + H]$^+$; HRMS (ESI) calculated for $C_{32}H_{32}N_5O_3$: 534.2505 [M + H]$^+$, found 534.2507; ; HPLC purity (method A): 98.9%, t_R = 22.72 min.

***N*-[3-(4-{[(1*S*)-2-Hydroxy-1-phenylethyl]amino}-6-phenylthieno[2,3-*d*]pyrimidin-5-yl)phenyl]prop-2-enamide (85).** Compound **85** was prepared from acryloyl chloride and **69**, similarly to **70**. After work-up, the residue was purified by preparative layer chromatography (ethyl acetate/hexanes = 1:1) to give the product **85** (67 mg, 68%). ^{1}H NMR (300 MHz, $CDCl_3$): δ 8.90 (s, 1H, NH), 8.30–8.27 (m, 1H), 7.80–7.46 (m, 2H), 7.39–7.10 (m, 9H), 7.08–7.00 (m,

1H), 6.94–6.90 (m, 2H), 6.45–6.16 (m, 2H), 5.71–5.54 (m, 1H), 5.32–5.15 (m, 1H), 3.82–3.52 (m, 2H); ^{13}C NMR (75 MHz, $CDCl_3$) δ 164.9, 164.8, 164.4, 163.3, 157.1, 157.0, 153.4, 153.0, 139.2, 138.9, 138.8, 138.3, 136.8, 136.5, 136.3, 136.1, 132.9, 132.8, 130.8, 130.5, 130.2, 129.4, 129.3, 128.9, 128.8, 128.6, 128.5, 128.2, 128.1, 128.1, 127.9, 127.6, 127.0, 126.3, 122.7, 121.5, 120.7, 120.0, 116.4, 68.0, 67.0, 58.3, 56.9; LC-MS (ESI) *m/z* 493.1 $[M + H]^+$; HRMS (ESI) calculated for $C_{29}H_{24}N_4O_2SNa$: 515.1518 $[M + Na]^+$, found 515.1526; HPLC purity (method A): 99.4%, t_R = 35.28 min.

Docking analysis of compound 2 with EGFR protein

The protein structures of EGFR (Protein Data Bank identifier (PDB ID: 4JQ7)[32] was apply for this study. The docking analysis was conducted by using the CovalentDock[57] program with the CHARMm force field.[58] The number of docking poses was set as 20 with default parameters. The decision of the best pose was according to the lowest binding energy of the compound will form a covalent bond with Cys797 and hinge binding with Met793.

X-ray Co-crystal Study of Wild-Type EGFR Kinase in Complex with 78

Wild-type human EGFR (residues 696-1022) was constructed and expressed in High Five insect cells. Protein purification and crystallization was performed as described[32]. EGFR/**78** complex crystal was obtained by soaking apo form crystal with **78** in reservoir solution containing 0.6 mM compound for 5−6 hour at room temperature. Data for complex structure was collected at NSRRC (beamline BL13C1) at 100K and processed using HKL2000.[59] Model

building and structure determinations were carried out as previously described[28,32] except that structural refinement was done by program PHENIX.[60] The data collection and refinement statistics of EGFR/78 complex crystal was summary in supporting information.

Biology

Reagents, materials, plasmids, and cell lines (with name, manufacturer)

For the baculoviral expression vector of GST-tagged EGFR kinase domain (GST-EGFR-KD, L858R/T790M), the PCR-amplified cDNA fragment covering human EGFR from amino acids 696 to 1022 was attached to the C-terminal coding region (30 region) of the glutathione S-transferase gene. The fused DNA fragment was cloned into a baculovirus expression vector pBacBAK8 (Clontech, Palo Alto, CA, USA). H1975 cell lines were obtained from the American Type Culture Collection (ATCC, USA) and they were grown in RPMI 1640 (ATCC, USA) with 10% fetal bovine serum (FBS) (Gibco, USA). EGFR L858R/T790M (DM) substrate peptide (GGMEDIYFEFMGGKKK) (GMbiolab), HEPES (Gene Mark, 7365-45-9), $MnCl_2$ (JT Baker), $MgCl_2$ (Sigma-Aldrich, M8260), Triton X-100 (Sigma-Aldrich), Dithiothreitol (DTT, MDBio, Inc), Bovine Serum Albumin (BSA, Sigma-Aldrich), Sodium Orthovanadate (Na_3VO_4) (Sigma-Aldrich), Poly (Glu, Tyr) sodium salt Glu: Tyr (4:1) (Sigma-Aldrich), ATP (Sigma-Aldrich), 96 well microplates (Greiner Bio One), Black 96 well microplate (SPL), Plate sealers (Basic Life), Wallac 1420 Victor 2 multilabel counter (PerkinElmer), Kinase-Glo Plus Luminescent Kinase Assays (Promega).

Purified kinase confirmatory activity assay for EGFR wild-type, EGFR L858R, and EGFR L858R/T790M

Kinase-Glo Plus Luminescent Kinase Assays (Promega) was used to test the kinase activities of GST-EGFR (G696-G1022) wild-type, L858R, and L858R/T790M double-mutant recombinant proteins. The assay was performed in round bottom 96-well microplate in a final volume of 50 μL containing the following components: 50 ng wild-type EGFR, 50 ng single-mutant EGFR or 200 ng double-mutant EGFR, 25 mM HEPES pH 7.4, 4 mM $MnCl_2$, 2 mM DTT, 10 mM $MgCl_2$, 0.01% BSA, 0.02% Triton X-100, 0.5 mM Na_3VO_4, 2 μM poly (Glu, Tyr) 4:1 (for wild-type EGFR and single-mutant EGFR) or 25 μM EGFR L858R/T790M substrate peptide (for double-mutant EGFR), 1–5 μM ATP, and varying concentrations of the tested compounds. After incubation at 37 °C for 60 min (for wild-type EGFR) or 30 °C for 120 min (for single- and double-mutant EGFR), 50 μL Kinase-Glo Plus reagent was added to each well of the black microplate and placed in the dark for 10 min at room temperature. Finally, the luminescence was measured on a Wallac 1420 Victor2 multilabel counter (PerkinElmer). Data were normalized using DMSO-only controls and background controls (no kinase added) to verify compound inhibition. The IC_{50} value was calculated using GraphPad Prism version 4 software (San Diego, CA, USA).

Cellular proliferation assays

The proliferation assays were performed by seeding 3,000 cells per well in a 96-well culture plate. After 16 hours, cells were treated with vehicle or test compounds at various concentrations of the tested compound in medium for 96 hours. Cell viability was quantitated using the MTS method (Promega, Madison, WI, USA) according to the manufacturer's recommended protocol. Results were determined by measuring the absorbance at 490 nm using a plate reader (PowerWave X; BioTek Instruments, Inc., USA). The CC_{50} value was defined as the amount of compound that caused 50% reduction in cell viability in comparison with DMSO-treated (vehicle) control and was calculated using GraphPad Prism version 4 software (GraphPad, USA).

Data analysis

For Kinase-Glo kinase assays, the measured data were normalized using DMSO-only controls (0% inhibition) and background controls (100% inhibition) to verify inhibition by the compounds. The IC_{50} value was defined as the amount of compound that induced a 50% inhibition in enzyme activity in comparison with DMSO-treated controls and was calculated using GraphPad Prism version 4 software. Z0 values were calculated using the method of Zhang et al.[61]

In vivo antitumor efficacy studies in HCC827 human lung cancer xenograft model.

The antitumor activity of orally gavaged compounds formulated in several vehicles was measured in HCC827 (Del E746_A750 in exon19) tumor bearing male nude mice (6- to 8-

week-old athymic NU-Fox1^{nu} nude mice from BioLASCO, Taiwan). Each mouse was inoculated subcutaneously at the left flank region with HCC827 tumor cells (5x10^6 cells/mouse). Oral gavages treatment was started when the mean tumor size reached approximately 500 mm^3. **78** prepared in vehicle 1 (1% methylcellulose-4000cps/0.5% Tween 80/98.5% H_2O) was orally gavaged at dose levels of 10, 20 and 50 mg/kg to the tumor bearing mice once a day, 5 days a week for 2 consecutive weeks.

In vivo antitumor efficacy studies in NCI-H1975 human lung cancer xenograft model.

The antitumor efficacy studies of the compounds were examined by CrownBio Inc. 52.5 mg of **78** powder were weighed and dissolved with 10.5 mL of vehicle (1% MC, 0.5% Tween 80) and mixed well by vortexing or sonication. The NCI-H1975 tumor cells were maintained *in vitro* as a monolayer culture in RPMI1640 medium supplemented with 10% heat-inactivated fetal bovine serum at 37 ºC in an atmosphere of 5% CO_2 in air. The tumor cells were routinely subcultured twice weekly by trypsin-EDTA treatment. Cells in exponential growth phase were harvested and counted for tumor inoculation. Each BALB/c nude mice was inoculated subcutaneously at the right flank region with NCI-H1975 tumor cells (5 x 10^6) in 0.1 ml of PBS for tumor development. Treatments were started when the mean tumor size reached 147 mm^3. The test article was administered to the tumor-bearing mice (n = 5/compound) according to the predetermined regimen for 15 days (QD). The date of tumor cell inoculation is denoted as day 0. TGI (%) is an indication of antitumor effectiveness and it is defined as TGI (%) =100 x

(1−T/C). T and C were the mean tumor volume of the treated and control groups, respectively. Tumor volumes were measured in two dimensions using a caliper, and the volume was expressed in mm^3 using the formula: $V = 0.5\ a \times b^2$ where a and b are the major and minor diameters of the tumor, respectively. Studies were reviewed and approved by the Institutional Animal Care and Use Committee (IACUC) of CrownBio prior to conduct. During the study, care and use of animals was conducted in accordance with the regulations of the Association for Assessment and Accreditation of Laboratory Animal Care (AAALAC).

ASSOCIATED CONTENT

Supporting information

Molecular formula strings of the final compounds, supplementary methods, and general procedures for the preparation of the compounds are available free of charge via the Internet at http://pubs.acs.org.

Accession Codes

PDB ID for EGFR wild-type with compound **78** is 6JZ0. Authors will release the atomic coordinates and experimental data upon article publication.

AUTHOR INFORMATION

Corresponding Author information

Hsing-Pang Hsieh, E-mail: hphsieh@nhri.org.tw.

Phone: +886-37-246-166 extension 35708.

Fax: +886-37-586-456

Notes

The authors declare no competing financial interest.

ACKNOWLEDGMENTS

Support from the National Health Research Institute and Ministry of Science and Technology, Taiwan (MOST 106-2113-M-400-001 and MOST 105-2325-B-400-010 for H.P.H.) is acknowledged. This work is also financially supported by the Center of Applied Nanomedicine, National Cheng Kung University from The Featured Areas Research Center Program within the framework of the Higher Education Sprout Project by the Ministry of Education (MOE) in Taiwan. S.Y.L. is supported by a postdoctoral fellowship from Ministry of Science and Technology, Taiwan. We thank Dr. Vincent Blay for help with English editing.

ABBREVIATIONS USED

EGFR, epidermal growth factor receptor; NSCLC, non-small cell lung cancer; SCLC, small cell lung cancer; ATP, adenosine triphosphate; FDA, food and drug administration; TKI, tyrosine kinase inhibitor; DFG, Asp-Phe-Gly; SBDD, structure-based drug design; SAR, structure-activity relationship; IND, investigational new drug; EDCI·HCl, 1-(3-dimethylaminopropyl)-3-ethylcarbodiimide hydrochloride; TBAF, tetrabutylammonium fluoride; HRD, His-Arg-Asp; PK, pharmacokinetic; AUC, area under curve; TGI, tumor growth inhibition; QD, once a day.

REFERENCES

(1) World Health Organization (WHO) Statistics Reports for Lung Cancer. http://www.who.int/news-room/fact-sheets/detail/cancer (assessed Feb 1, 2018).

(2) Jemal, A.; Bray, F.; Center, M. M.; Ferlay, J.; Ward, E.; Forman, D. Global cancer statistics. *CA Cancer J. Clin.* **2011**, *61*, 69–90.

(3) Sharma, S. V.; Bell, D. W.; Settleman, J.; Haber, D. A. Epidermal growth factor receptor mutations in lung cancer. *Nat. Rev. Cancer* **2007**, *7*, 169–181.

(4) Prabhakar, C. N. Epidermal growth factor receptor in non-small cell lung cancer. *Transl. Lung Cancer Res.* **2015**, *4*, 110–118.

(5) Shi, Y.; Au, J. S. K.; Thongprasert, S.; Srinivasan, S.; Tsai, C. M.; Khoa, M. T.; Heeroma, K.; Itoh, Y.; Cornelio, G.; Yang, P. C. A prospective, molecular epidemiology study of EGFR mutations in asian patients with advanced non-small-cell lung cancer of adenocarcinoma histology (PIONEER). *J. Thorac. Oncol.* **2014**, *9*, 154–162.

(6) Chan, D. L. H.; Segelov, E.; Wong, R. S. H.; Smith, A.; Herbertson, R. A.; Li, B.T.; Tebbutt, N.; Price, T.; Pavlakis, N. Epidermal growth factor receptor (EGFR) inhibitors for metastatic colorectal cancer. *Cochrane Database Syst. Rev.* **2017**, *6*, CD007047.

(7) Tan, C. S.; Cho, B. C.; Ross. A. S. Next-generation epidermal growth factor receptor tyrosine kinase inhibitors in epidermal growth factor receptor -mutant non-small cell lung cancer. *Lung Cancer* **2016**, *93*, 59–68.

(8) Muhsin, M.; Graham, J.; Kirkpatrick, P. Gefitinib. *Nat. Rev. Drug Discov.* **2003**, *2*, 515–516.

(9) Cohen, M. H.; Johnson, J. R.; Chen, Y. F.; Sridhara, R.; Pazdur, R. FDA drug approval summary: erlotinib (Tarceva®) tablets. *Oncologist* **2015**, *10*, 461–466.

(10) Peters, S.; Zimmermann, S.; Adjei, A. A. Oral epidermal growth factor receptor tyrosine kinase inhibitors for the treatment of non-small cell lung cancer: comparative pharmacokinetics and drug–drug interactions. *Cancer Treat. Rev.* **2014**, *40*, 917–926.

(11) Molina, J. R.; Yang, P.; Cassivi, S. D.; Schild, S. E.; Adjei, A. A. Non–small cell lung cancer: epidemiology, risk factors, treatment, and survivorship. *Mayo Clin. Proc.* **2008**, *83*, 584–594.

(12) Pao, W.; Miller, V. A.; Politi, K. A.; Riely, G. J.; Somwar, R.; Zakowski, M. F.; Kris, M. G.; Varmus, H. Acquired resistance of lung adenocarcinomas to gefitinib or erlotinib is associated with a second mutation in the EGFR kinase domain. *PLoS Med.* **2005**, *2*, e73.

(13) Huang, L.; Fu, L. Mechanisms of resistance to EGFR tyrosine kinase inhibitors. *Acta Pharmaceutica Sinica B* **2015**, *5*, 390–401.

(14) Nelson, V.; Ziehr, J.; Agulnik, M.; Johnson, M. Afatinib: emerging next-generation tyrosine kinase inhibitor for NSCLC. *Onco. Targets Ther.* **2013**, *6*, 135–143.

(15) Dungo, R. T.; Keating, G. M. Afatinib: first global approval. *Drugs* **2013**, *73*, 1503–1515.

(16) U. S. Food and Drug Administration, FDA Broadens Afatinib Indication to Previously

Untreated, Metastatic NSCLC with Other Non-Resistant EGFR Mutations. https://www.fda.gov/drugs/informationondrugs/approveddrugs/ucm592558.htm (accessed Jan 16, 2018).

(17) Sullivan, I.; Planchard, D. Next-generation EGFR tyrosine kinase inhibitors for treating EGFR-mutant lung cancer beyond first line. *Frontiers in Medicine* **2017**, *3*, 76.

(18) Han, W.; Du, Y. Recent development of the second and third generation irreversible epidermal growth factor receptor inhibitors. *Chem. Biodivers.* **2017**, *14*, e1600372.

(19) U. S. Food and Drug Administration, Osimertinib (TAGRISSO). https://www.fda.gov/drugs/informationondrugs/approveddrugs/ucm549683.htm. (accessed Jul 28, 2017)

(20) Finlay, M. R. V.; Anderton, M.; Ashton, S.; Ballard, P.; Bethel, P. A.; Box, M. R.; Bradbury, R. H.; Brown, S. J.; Butterworth, S.; Campbell, A.; Chorley, C.; Colclough, N.; Cross, D. A. E.; Currie, G. S.; Grist, M.; Hassall, L.; Hill, G. B.; James, D.; James, M.; Kemmitt, P.; Klinowska, T.; Lamont, G.; Lamont, S. G.; Martin, N.; McFarland, H. L.; Mellor, M. J.; Orme, J. P.; Perkins, D.; Perkins, P.; Richmond, G.; Smith, P.; Ward, R. A.; Waring, M. J.; Whittaker, D.; Wells, S.; Wrigley, G. L. Discovery of a potent and selective EGFR inhibitor (AZD9291) of both sensitizing and T790M resistance mutations that spares the wild type form of the receptor. *J. Med. Chem.* **2014**, *57*, 8249–8267.

(21) U. S. Food and Drug Administration, FDA Approves Osimertinib for First-Line Treatment

of Metastatic NSCLC with Most Common EGFR Mutations. https://www.fda.gov/Drugs/InformationOnDrugs/ApprovedDrugs/ucm605113.htm (accessed Apr 19, 2018).

(22) Gao, X.; Le, X.; Costa, D. B. The safety and efficacy of osimertinib for the treatment of EGFR T790M mutation positive non-small-cell lung cancer. *Expert Rev. Anticancer Ther.* **2016**, *16*, 383–390.

(23) Tang, Z. H.; Lu, J. J. Osimertinib resistance in non-small cell lung cancer: mechanisms and therapeutic strategies. *Cancer Lett.* **2018**, *420*, 242–246.

(24) Russo, A.; Franchina, T.; Ricciardi, G. R. R.; Smiroldo, V.; Picciotto, M.; Zanghì, M.; Rolfo, C.; Adamo, V. Third generation EGFR TKIs in EGFR-mutated NSCLC: where are we now and where are we going. *Crit. Rev. Oncol. Hematol.* **2017**, *117*, 38–47.

(25) Lu, X.; Yu, L.; Zhang, Z.; Ren, X.; Smaill, J. B.; Ding, K. Targeting EGFRL858R/T790M and EGFRL858R/T790M/C797S resistance mutations in NSCLC: current developments in medicinal chemistry. *Med. Res. Rev.* **2018**, *38*, 1–32.

(26) U. S. Food and Drug Administration, FDA Approves Dacomitinib for Metastatic Non-Small Cell Lung Cancer. https://www.fda.gov/Drugs/InformationOnDrugs/ApprovedDrugs/ucm621967.htm (accessed Sep 28, 2018).

(27) Wu, Y. L.; Cheng, Y.; Zhou, X. Lee, K. H.; Nakagawa, K.; Niho, S.; Tsuji, F.; Linke, R.;

Rosell, R.; Corral, J.; Migliorino, M. R.; Pluzanski, A.; Sbar, E. I.; Wang, T.; White, J. L.; Nadanaciva, S.; Sandin, R.; Mok, T. S. Dacomitinib versus gefitinib as first-line treatment for patients with EGFR-mutation-positive non-small-cell lung cancer (ARCHER 1050): a randomised, open-label, phase 3 trial. *Lancet Oncol.* **2017**, *18*, 1454−1466.

(28) Coumar, M. S.; Chu, C. Y.; Lin, C. W.; Shiao, H. Y.; Ho, Y. L.; Reddy, R.; Lin, W. H.; Chen, C. H.; Peng, Y. H.; Leou, J. S.; Lien, T. W.; Huang, C. T.; Fang, M. Y.; Wu, S. H.; Wu, J. S.; Chittimalla, S. K.; Song, J. S.; Hsu, J. T.; Wu, S. Y.; Liao, C. C.; Chao, Y. S.; Hsieh, H. P. Fast-forwarding hit to lead: aurora and epidermal growth factor receptor kinase inhibitor lead identification. *J. Med. Chem*. **2010**, *53*, 4980−4988.

(29) Nagar, B. c-Abl tyrosine kinase and inhibition by the cancer drug imatinib (Gleevec/STI-571). *J. Nutr.* **2007**, *137*, 1518S–1523S.

(30) Hubbard, S. R. Crystal structure of the activated insulin receptor tyrosine kinase in complex with peptide substrate and ATP analog. *EMBO J.* **1997**, *16*, 5572–5581.

(31) Treiber, D. K.; Shah, N. P. Ins and outs of kinase DFG motifs. *Chem. Biol.* **2013**, *20*, 745–746.

(32) Peng, Y. H.; Shiao, H. Y.; Tu, C. H.; Liu, P. M.; Hsu, J. T. A.; Amancha, P. K.; Wu, J. S.; Coumar, M. S.; Chen, C. H.; Wang, S. Y.; Lin, W. H.; Sun, H. Y.; Chao, Y. S.; Lyu, P. C. Hsieh, H. P.; Wu, S.Y. Protein kinase inhibitor design by targeting the Asp-Phe-Gly (DFG) motif: the role of the DFG motif in the design of epidermal growth factor receptor

inhibitors. *J. Med. Chem*. **2013**, *56*, 3889–3903.

(33) Center of Drug Evaluation, Taiwan, Phase I Clinical Trial for DBPR112. http://www1.cde.org.tw/ct_taiwan/search_case2_tornado.php?caseno=2107 (accessed Jul 28, 2018).

(34) Karikios. D. J.; Boyer, M. J. Irreversible EGFR inhibitors in advanced non-small-cell lung carcinoma: rationale and clinical evidence. *Clin. Invest.* **2012**, *2*, 317–325.

(35) Ho, K. M.; Lam, C. H.; Luh, T. Y. Transition metal promoted reactions. Part 27. Nickel(II)-lithium aluminum hydride mediated reduction of carbon-sulfur bonds. *J. Org. Chem.* **1989**, *54*, 4474–4476.

(36) Coumar, M. S.; Tsai, M. T.; Chu, C. Y.; Uang, B. J.; Lin, W. H.; Chang, C. Y.; Chang, T. Y.; Leou, J. S.; Teng, C. H.; Wu, J. S.; Fang, M. Y.; Chen, C. H.; Hsu, J. T. A.; Wu, S. Y.; Chao, Y. S.; Hsieh, H. P. Identification, SAR studies, and x-ray co-crystallographic analysis of a novel furanopyrimidine aurora kinase an inhibitor. *ChemMedChem* **2010**, *5*, 255–267.

(37) Iyengar, R. R.; Judd, A. S.; Zhao, G.; Kym, P. R.; Sham, H. L.; Gu, Y.; Liu, G.; Liu, M.; Zhao, H.; Clark, R. F.; Frevert, E. U.; Cool, B. L.; Zhang, T.; Keyes, R. F.; Hansen, T. M.; Xin, Z. Thienopyridones as AMPK Activators for the Treatment of Diabetes and Obesity. U.S. Patent 2005/038068 A1, February 17, 2005.

(38) Dai, Y.; Guo, Y.; Frey, R. R.; Ji, Z.; Curtin, M. L.; Ahmed, A. A.; Albert, D. H.; Arnold,

L.; Arries, S. S.; Barlozzari, T.; Bauch, J. L.; Bouska, J. J.; Bousquet, P. F.; Cunha, G. A.; Glaser, K. B.; Guo, J.; Li, J.; Marcotte, P. A.; Marsh, K. C.; Moskey, M. D.; Pease, L. J.; Stewart, K. D.; Stoll, V. S.; Tapang, P.; Wishart, N.; Davidsen, S. K.; Michaelides, M. R.; Thienopyrimidine ureas as novel and potent multitargeted receptor tyrosine kinase inhibitors. *J. Med. Chem.* **2005**, *48*, 6066–6083.

(39) Beccalli, E. M.; Manfredi, A.; Marchesini, A. Alkynes from 5-aminoisoxazoles. *J. Org. Chem.* **1985**, *50*, 2372–2375.

(40) Tormyshev, V. M.; Trukhin, D. V.; Rogozhnikova, O. Y.; Mikhalina, T. V.; Troitskaya, T. I.; Flinn, A. Aryl alkyl ketones in a one-pot Gewald synthesis of 2-aminothiophenes. *Synlett* **2006**, *16*, 2559–2564.

(41) Therkelsen, F. D.; Rottländer, M.; Thorup, N.; Pedersen, E. B. 4-Metalated condensed pyrimidines: their preparation and reaction with aldehydes under Barbier-type conditions. *Org. Lett*. **2004**, *6*, 1991–1994.

(42) Capoferri, L.; Lodola, A.; Rivara, S.; Mor, M. Quantum mechanics/molecular mechanics modeling of covalent addition between EGFR-cysteine 797 and *N*-(4-anilinoquinazolin-6-yl) acrylamide. *J. Chem. Inf. Model.* **2015**, *55*, 589−599.

(43) Carmi, C.; Lodola, A.; Rivara, S.; Vacondio, F.; Cavazzoni, A.; Alfieri, R. R.; Ardizzoni, A.; Petronini, P. G.; Mor, M. Epidermal growth factor receptor irreversible inhibitors: chemical exploration of the cysteine-trap portion. *Mini-Rev. Med. Chem.*, **2011**, *11*, 1019–

1030.

(44) O'Kane, G. M.; Bradbury, P. A.; Feld, R.; Leighl, N. B; Liu, G.; Pisters, K.-M.; Kamel-Reid, S.; Tsao, M. S.; Shepherd, F. A. Uncommon EGFR mutations in advanced non-small cell lung cancer. *Lung Cancer* **2017**, *109*, 137−144.

(45) Arcila, M. E.; Nafa, K.; Chaft, J. E.; Rekhtman, N.; Lau, C.; Reva, B. A.; Zakowski, M. F.; Kris, M. G.; Ladanyi M. EGFR exon 20 insertion mutations in lung adenocarcinomas: prevalence, molecular heterogeneity, and clinicopathologic characteristics. *Mol. Cancer. Ther.* **2013**, *12*, 220−229.

(46) Oxnard, G. R.; Lo, P. C.; Nishino, M.; Dahlberg, S. E.; Lindeman, N. I.; Butaney, M.; Jackman, D. M.; Johnson, B. E.; Jänne, P. A. Natural history and molecular characteristics of lung cancers harboring EGFR exon 20 insertions. *J. Thorac. Oncol.* **2013**, *8*, 179–184.

(47) Yang, M.; Xu, X.; Cai, J.; Ning, J.; Wery, J. P.; Li, Q.-X. NSCLC harboring EGFR exon-20 insertions after the regulatory C-helix of kinase domain responds poorly to known EGFR inhibitors. *Int. J. Cancer* **2016**, *139*, 171−176.

(48) Li, B. T.; Ross, D. S.; Aisner, D. L.; Chaft, J. E.; Hsu, M.; Kako, S. L.; Kris, M. G.; Varella-Garciam, M.; Arcila, M. E. HER2 amplification and HER2 mutation are distinct molecular targets in lung cancers. *J. Thorac. Oncol.* **2016**, *11*, 414–419.

(49) U.S. National Library of Medicine, ClinicalTrials.gov. https://clinicaltrials.gov/ct2/show/NCT03066206 (accessed Mar 15, 2019).

(50) U.S. National Library of Medicine, ClinicalTrials.gov. https://clinicaltrials.gov/ct2/show/NCT02716116 (accessed Mar 15, 2019).

(51) Robichaux, J. P.; Elamin, Y. Y.; Tan, Z.; Carter, B. W.; Zhang, S.; Liu, S.; Li, S.; Chen, T.; Poteete, A.; Estrada-Bernal, A.; Le, A. t.; Truini, A.; Nilsson, M. B.; Sun, H.; Roarty, E.; Goldberg, S. B.; Brahmer, J. R.; Altan, M.; Lu, C.; Papadimitrakopoulou, V.; Politi, K.; Doebele, R. C.; Wong, K.-K.; Heymach, J. V. Mechanisms and clinical activity of an EGFR and HER2 exon 20 selective kinase inhibitor in non–small cell Lung cancer. *Nat. Med.* **2018**, *24*, 638–646.

(52) Heymach, J. V.; Negrao, M.; Robichaux, J.; Carter, B.; Patel, A.; Altan, M.; Gibbons, D.; Fossella, F.; Simon, G.; Lam, V.; Blumenschein, G.; Tsao, A.; Kurie, J.; Mott, F.; Jenkins, D.; Mack, D.; Feng, L.; Roeck, B.; Yang, Z; Papadimitrakopoulou, V.; Elamin, A. A phase II trial of poziotinib in EGFR and HER2 exon 20 mutant non-small cell lung cancer (NSCLC). *J. Thorac. Oncol.* **2018**, *13*, S323−S324.

(53) Reaction Biology Corporation Home Page. http://www.reactionbiology.com/webapps/site/KinaseAssay.aspx (accessed Jan 6, 2019).

(54) Fabbro, D.; Cowan-Jacob, S. W.; Moebitz, H. Ten things you should know about protein kinases: IUPHAR review 14. *Br. J. Pharmacol.* **2015**, *172*, 2675−2700.

(55) Hasenahuer, M. A.; Barletta, G. P.; Fernandez-Alberti, S.; Parisi, G.; Fornasari, M. S. Pockets as structural descriptors of EGFR kinase conformations. *PLoS One* **2017**, *12*,

e0189147.

(56) Songtawee, N.; Gleeson, P.; Choowongkomon, K. Computational study of EGFR inhibition: molecular dynamics studies on the active and inactive protein conformations. *J. Mol. Model* **2013**, *19*, 497−509.

(57) Ouyang, X.; Zhou, S.; Su, C. T. T.; Ge, Z.,; Li, R; Kwoh, C. K. CovalentDock: automated covalent docking with parameterized covalent linkage energy estimation and molecular geometry constraints. *J. Comput. Chem.* **2013**, *34*, 326–336.

(58) Brooks, B. R.; Brooks, C. L. 3rd; Mackerell, A. D. Jr.; Nilsson, L.; Petrella, R. J.; Roux, B.; Won, Y.,; Archontis, G.; Bartels, C.; Boresch, S.; Caflisch, A.; Caves, L.; Cui, Q.; Dinner, A. R.; Feig, M.; Fischer, S.; Gao, J.; Hodoscek, M.; Im, W.; Kuczera, K.; Lazaridis, T.; Ma, J.; Ovchinnikov, V.; Paci, E.; Pastor, R. W.; Post, C. B.; Pu, J. Z.; Schaefer, M.; Tidor, B.; Venable, R. M.; Woodcock, H. L.; Wu, X.; Yang, W.; York, D. M.; Karplus, M. CHARMM: the biomolecular simulation program. *J. Comput. Chem.* **2009**, *30*, 1545–1614.

(59) Otwinowski, Z.; Minor, W. Processing of X-ray Diffraction Data Collected in Oscillation Mode. In *Methods in Enzymology*; Carter, C.W. Jr., Ed.; Academic: New York, 1997; Vol. 276, pp307–326.

(60) Adams, P. D.; Afonine, P. V.; Bunkóczi, G.; Chen, V. B.; Davis, I. W.; Echols, N.; Headd, J. J.; Hung, L.-W.; Kapral, G. J.; Grosse-Kunstleve, R. W.; McCoy, A. J.; Moriarty, N. W.; Oeffner, R.; Read, R. J.; Richardson, D. C.; Richardson, J. S.; Terwilliger, T. C.; Zwart, P.

H. PHENIX: a comprehensive python-based system for macromolecular structure solution. *Acta Cryst.* **2010**, *66*, 213–221.

(61) Zhang, J. H.; Chung, T. D. Y.; Oldenburg. K. R. A simple statistical parameter for use in evaluation and validation of high throughput screening assays. *J. Biomol. Screen* **1999**, *4*, 67–73.

Table of Contents Graphic.